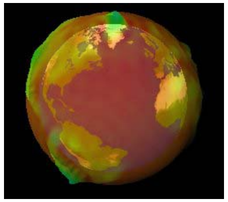

Computational Visualization

1. Sources, characteristics, representation

2. Mesh Processing

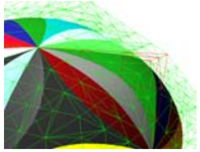

3. Contouring

4. Volume Rendering

5. Flow, Vector, Tensor Field Visualization

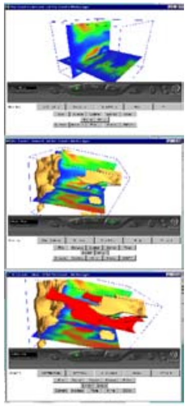

6. Application Case Studies

Computational Visualization:

Flow, Vector, Tensor Field Visualization

Lecture 5

Outline:
Scalar and Vector Topology

- I PROBLEM DOMAIN
- Scalar Fields ---- restrictions to surfaces
- Vector Fields ---- extensions to functions
  on surfaces
- Different Grids --- unstructured, curvilinear
- II TOPOLOGY COMPUTATION
- Critical Points --- nonlinear system solvers; multiplicity, index
- Local Analysis --- eigenvalues, newton factorization
- Streamlines --- advection; dual stream surfaces

Interrogation of Axial Vortices

(with G. Blaisdell, Purdue University)

- How is the turbulent kinetic energy produced ?
- Are the production terms of kinetic energy related to the large helical vortices ?
- Do the helical vortices rotate, move axially or remain stationary?

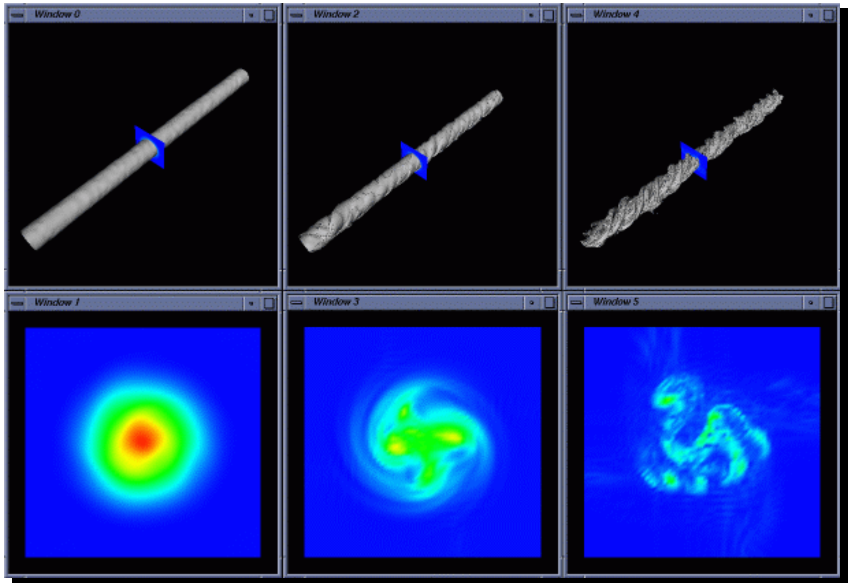

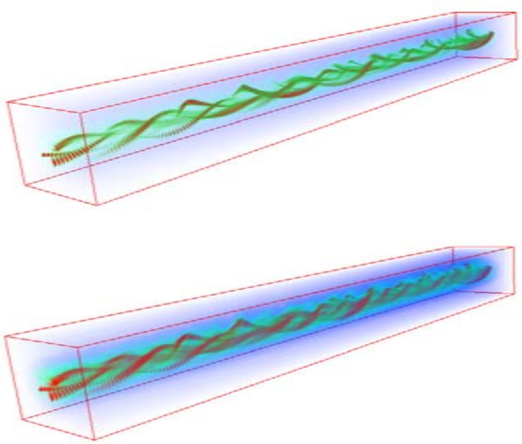

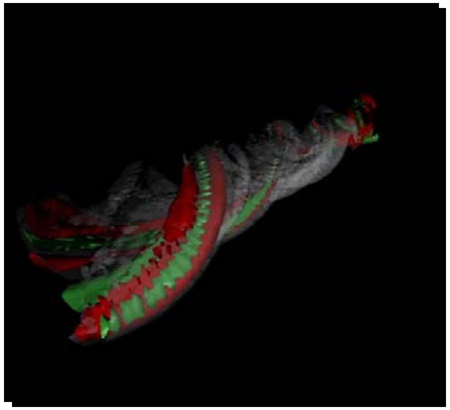

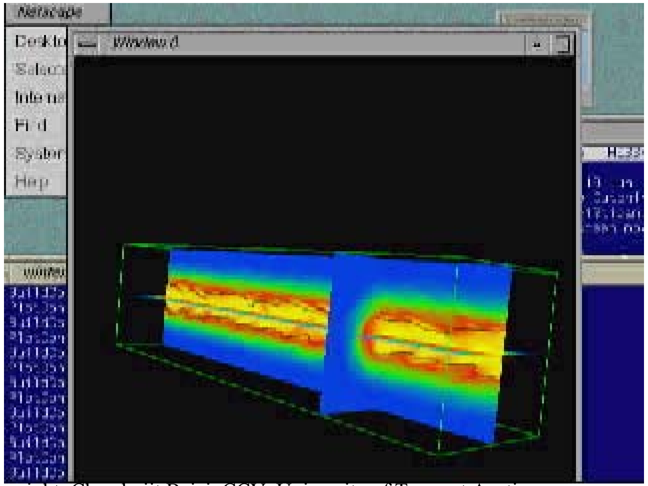

Line Integral Convolution

- **Input** vector field and texture (white noise)
- **Output** intensity value on each pixel
- Output image is highly correlated along the streamlines and uncorrelated in directions perpendicular to the streamlines

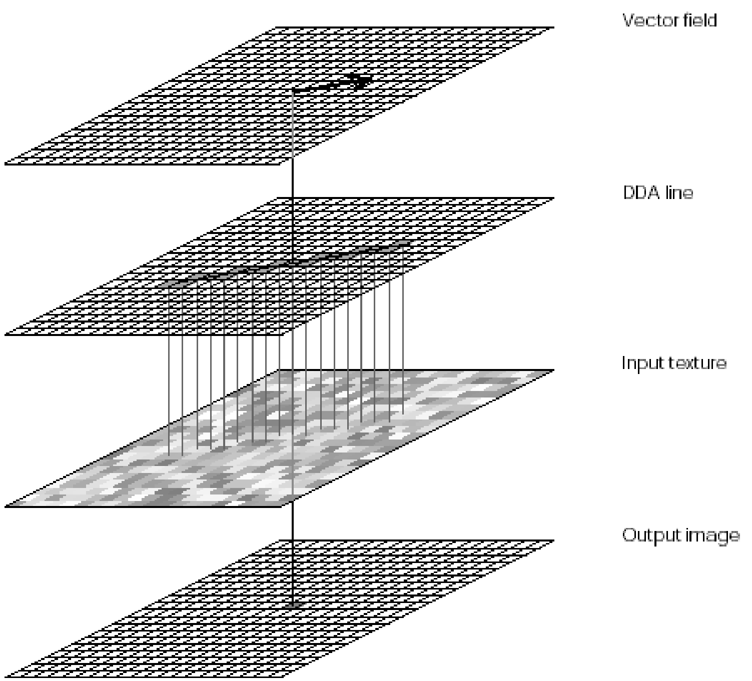

Line Integral Convolution

- Given a vector field $\vec{v}$, the streamline equation is

$$\frac{d\vec{\sigma}(s)}{ds} = \frac{d\vec{\sigma}}{dt}\frac{dt}{ds} = \frac{\vec{v}}{\|v\|}$$

Image intensity at a point $\vec{x}$ is defined as

$$I(\vec{x}) = \int_{s_0 - L}^{s_0 + L} T(\vec{\sigma}(s))k(s - s_0)ds$$

where T is the input white noise texture and $\vec{\sigma}(s)$ is the streamline with $\vec{\sigma}(s_0) = \vec{x}$

$k(s)$ is a symmetric filter function.

LIC Example

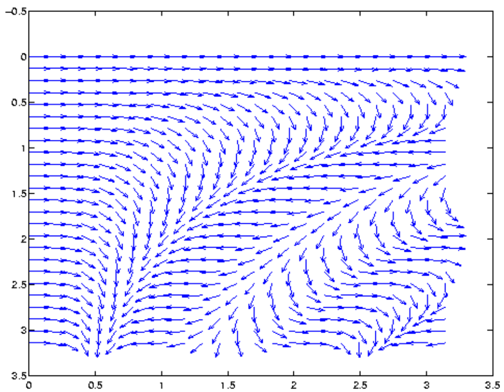

Input vector field

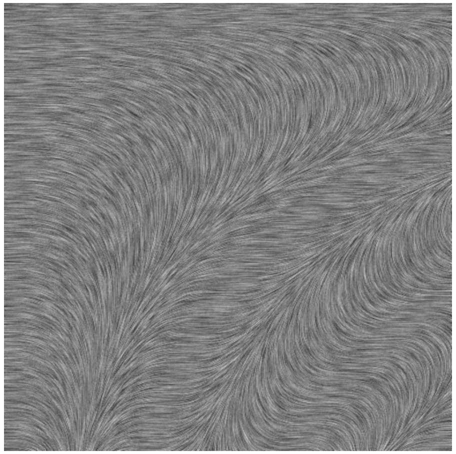

L=20

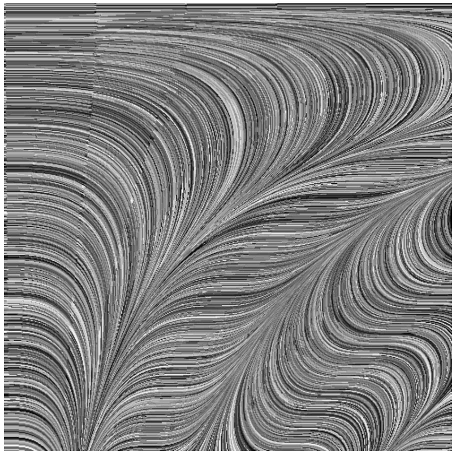

L=200

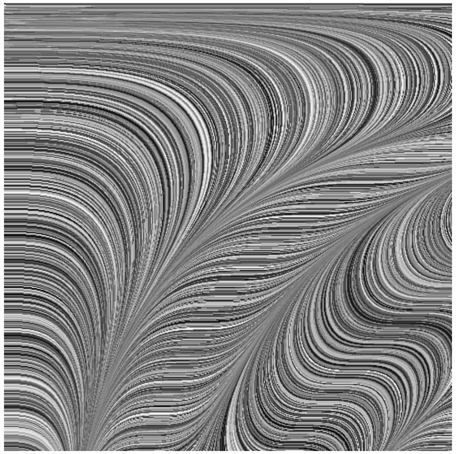

L=800

Double LIC

- Original LIC
  - Random white noise values averaged along a local streamline.
  - Flow lines not delineated clearly
- Double LIC
  - Use the output image of first LIC as the input of the second LIC
  - Pixel intensities averaged along a previously integrated streamline.

Enhanced LIC

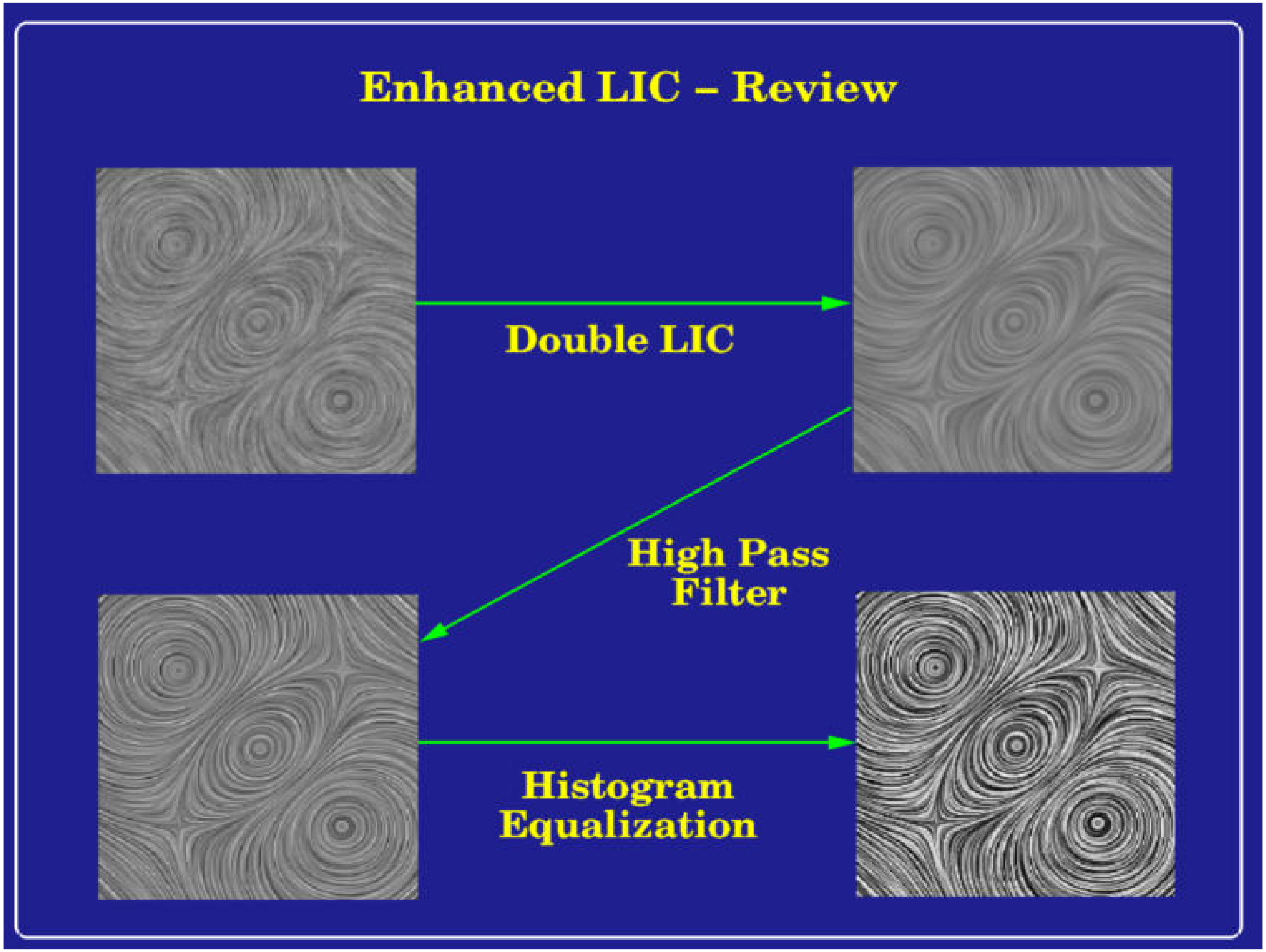

Vector Signature Function

- Given two scalar fields $U(x, y, z)$, $V(x, y, z)$ defined over a 3D volume,
- Inner Volume

$$I(u, v) = Volume(U(x, y, z) <= u \text{ and } V(x, y, z) <= v\})$$

- Outer Volume

$$O(x, y) = Volume(U(x, y, z) > u \text{ and } V(x, y, z) > v\}),$$

where u, v are called isovalues of U, V respectively.

- (I, O) is a vector field defined over the domain $\{U, V\}$. It is called a **vector signature function.**
- Vector signature function can be other properties of the two scalar fields.

Vector Signature Functions:Use of Vector Field Topology

- Consider two scalar fields F(x),   G(x)
- IF(w) is the region inside F(x)=w
- IG(w*) is the region inside G(x)=w*
- OF(w) is the region outside F(x)=w
- OG(w*) is the region outside G(x)=w*

- IV(w,w*) = Vol (IF(w) intersect IG(w*))
- OV(w,w*) = Vol (OF(w) intersect OG(w*))

- Vector field V defined in a 2D domain
- V(w,w*) = (IV,OV)

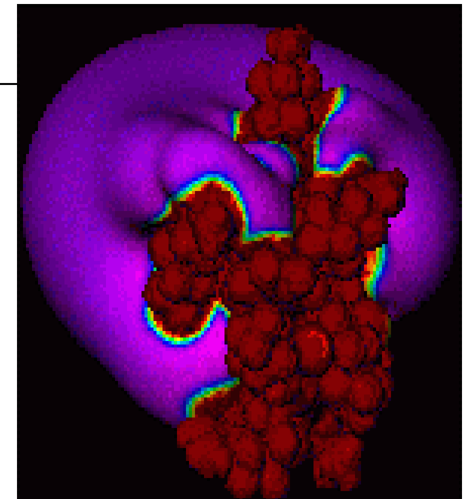

electrostatic

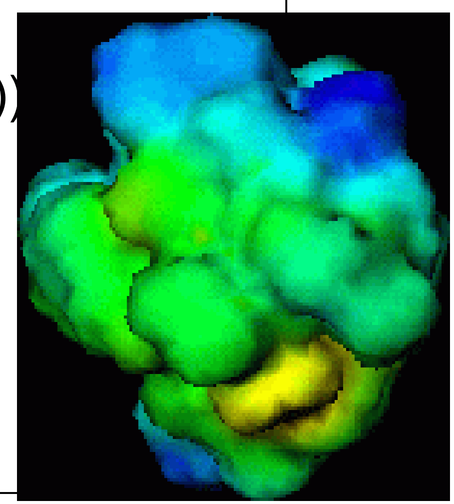

vanderWaal

Vector Correlation Signature Example

Glucose potentials (Electrostatics. vanderWaal)

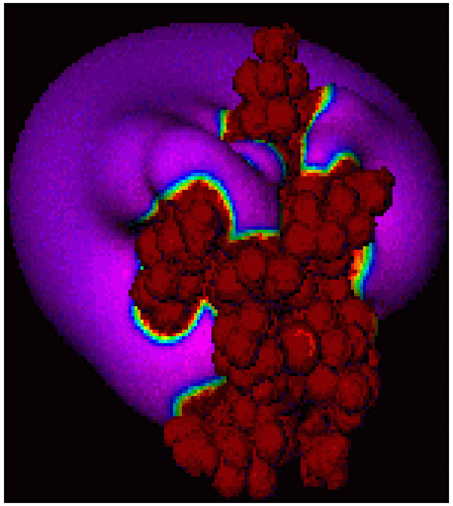

electrostatic

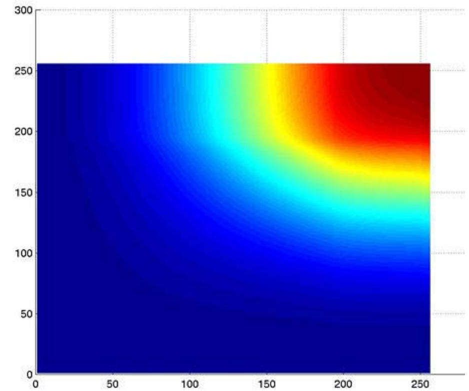

Inner volume

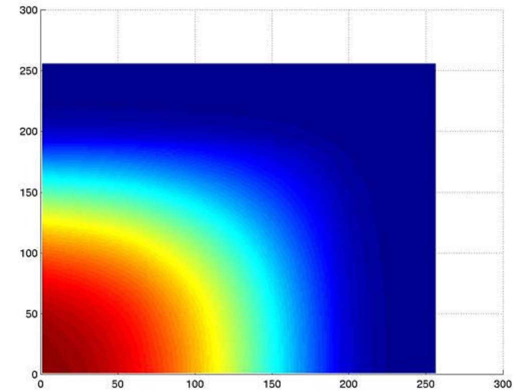

Outer volume

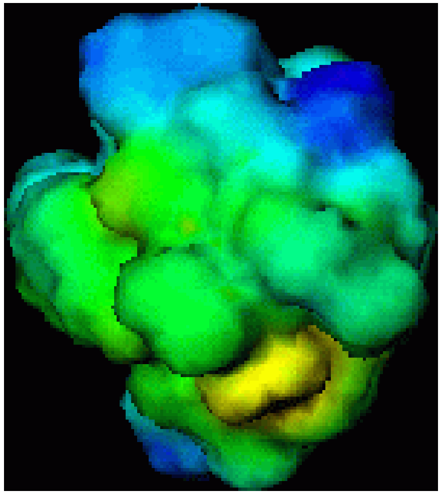

vanderWaal

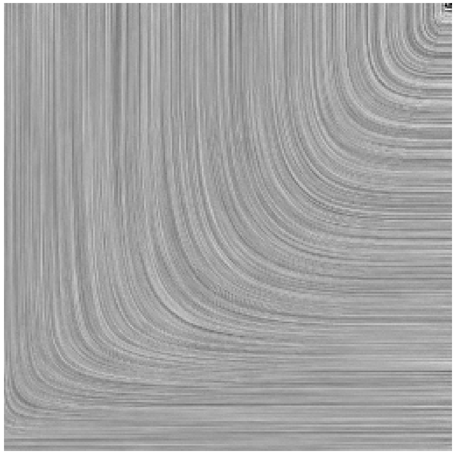

Single LIC

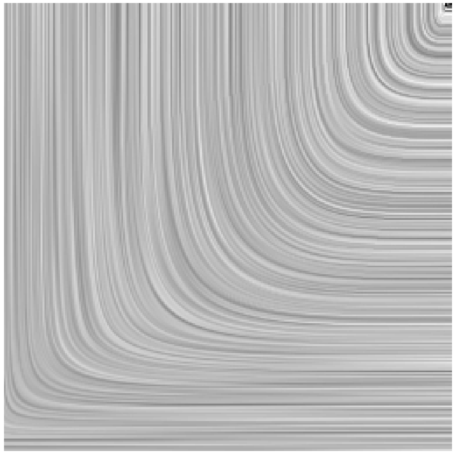

Double LIC

Construction of Vector Topology

- I Detect stationary (critical) points
- II Classify critical points
- III Link with integral curves of vector field

3D Vector Field

$$\left[f(x,y,z), \quad g(x,y,z), \quad h(x,y,z) \right]$$

Critical Points

$$\begin{bmatrix} f(x,y,z) \\ g(x,y,z) \\ h(x,y,z) \end{bmatrix} = 0$$

Eigenstructure of

First Order Local Analysis at the Critical Points

$$J = \begin{bmatrix} f_x & f_y & f_z \\ g_x & g_y & g_z \\ h_x & h_y & h_z \end{bmatrix}$$

Vector Local Topology (2D critical point classification)

Spiral Source
R + + I<>0

Saddle
R - - I=0

Source
R + + I =0

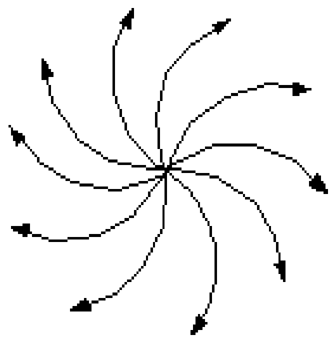

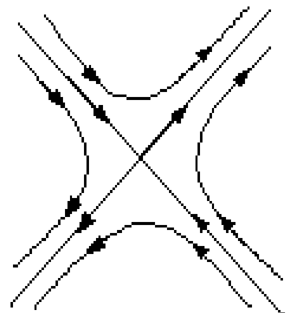

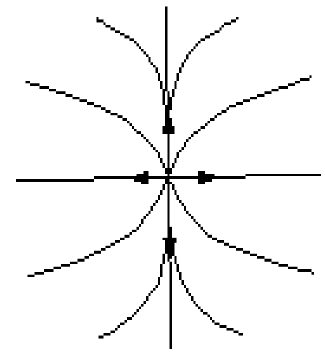

Spiral Source

Saddle

Source

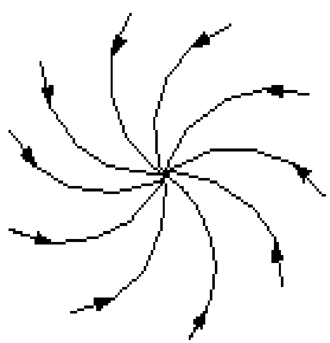

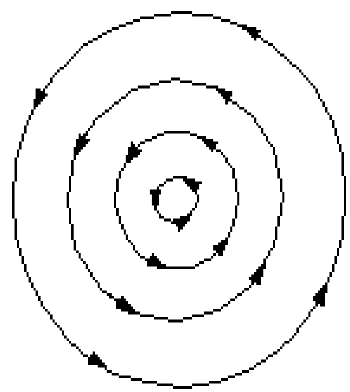

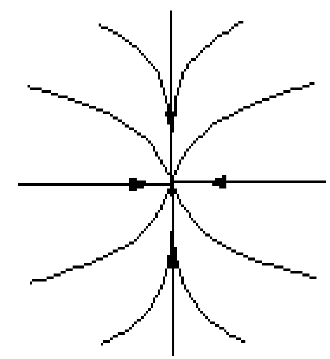

Spiral Sink
R - - I <>0

Center
R =0 I <>0

Sink
R - - I=0

Vortex Identification

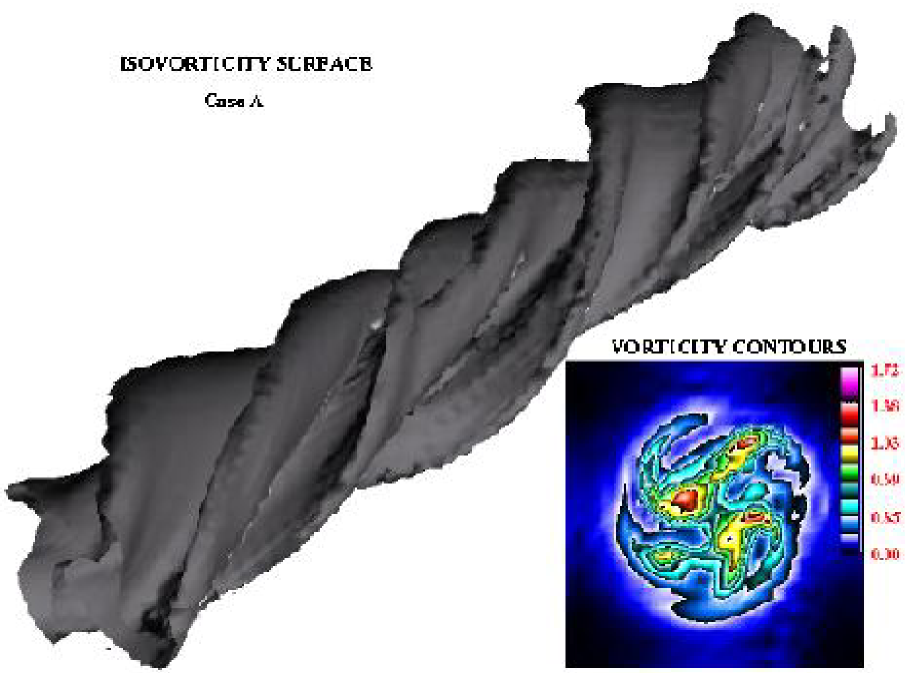

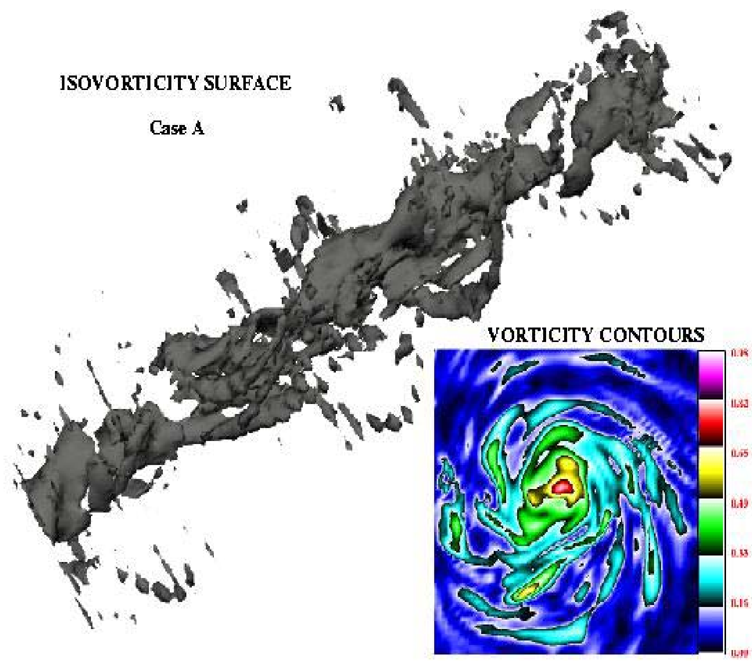

Vortex Core in Turbulent Flow

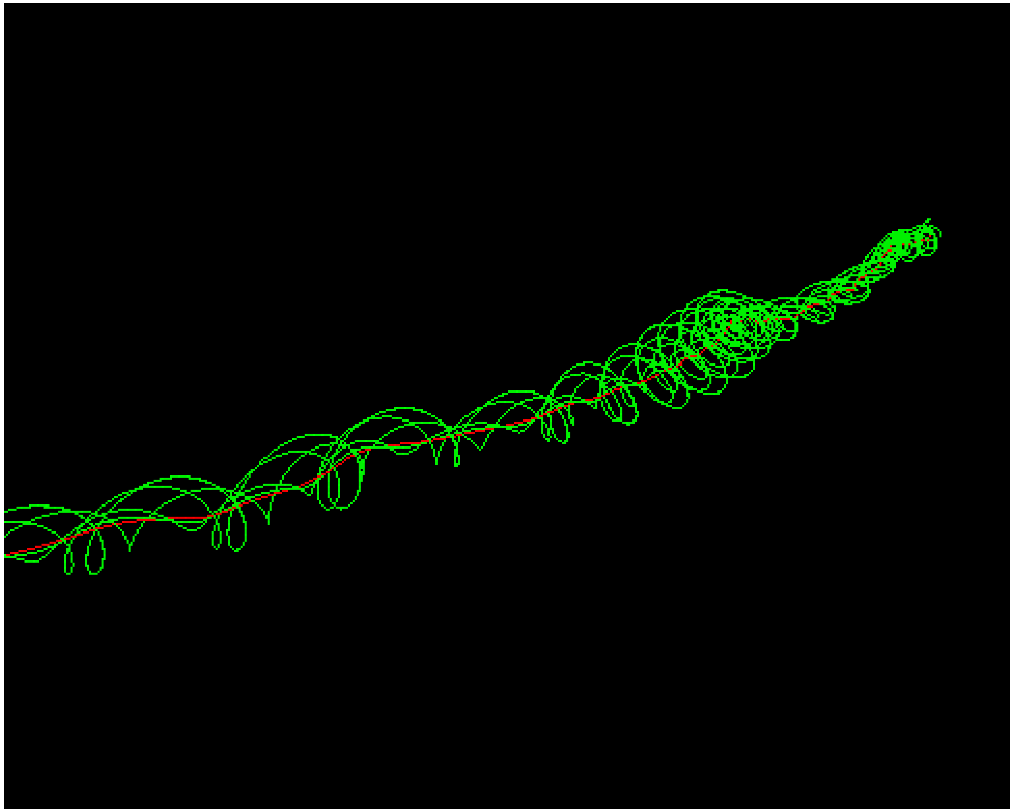

- Vortex core (red) computed by vector field topology. Green curves are streamlines computed near critical points on the vortex core.

Vector Field Visualization

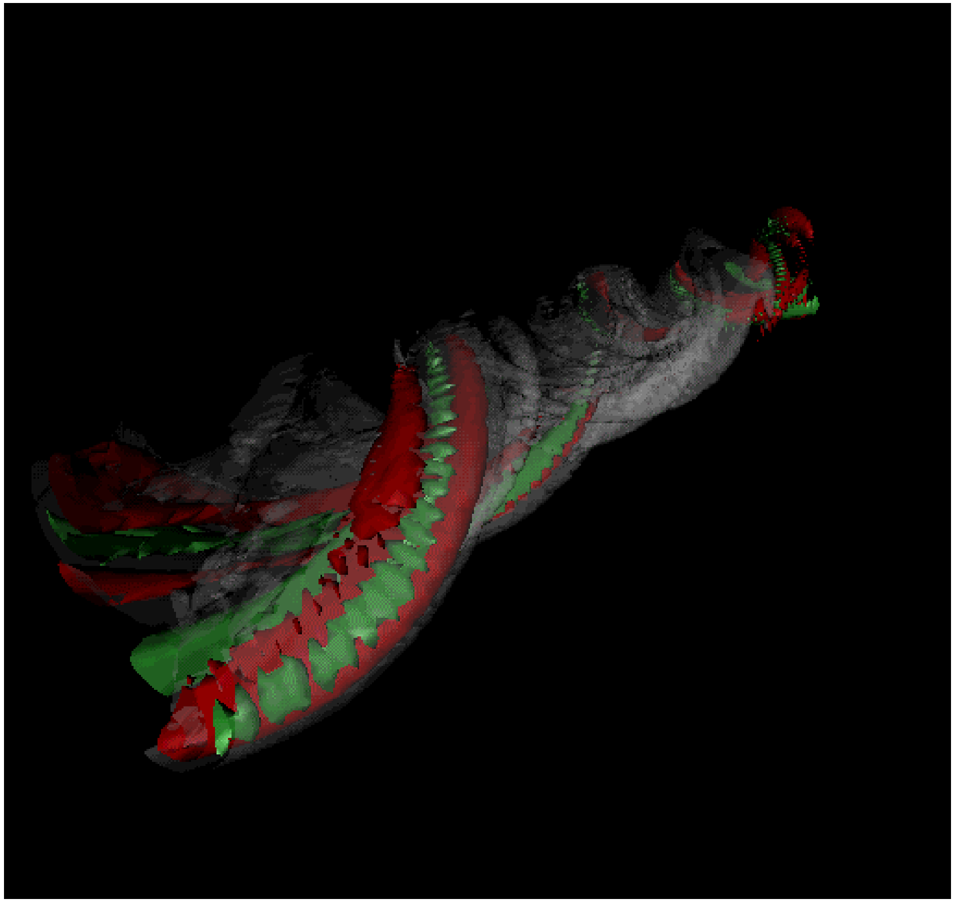

An isocontour of vorticity magnitude is displayed with partial transparency. The red contour represents a region of positive production term of turbulent kinetic energy. The green contour represents negative production terms.

Challenge: Detect Vortices, Topology Changes in Cosmological Explosions

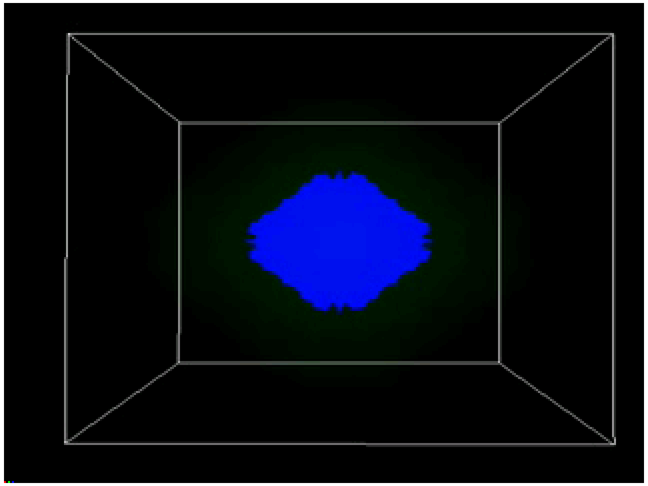

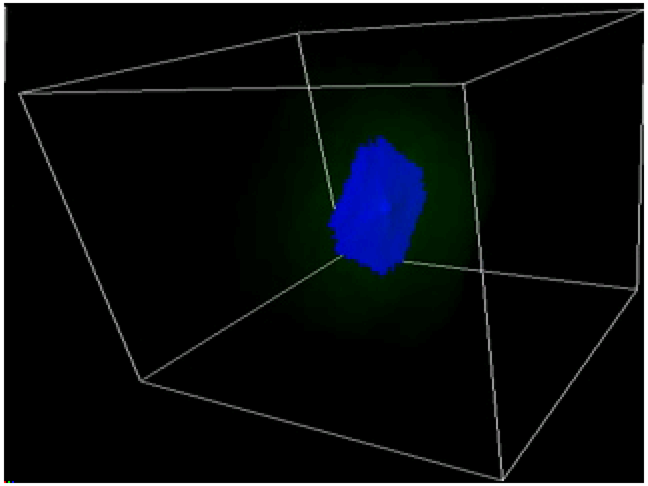

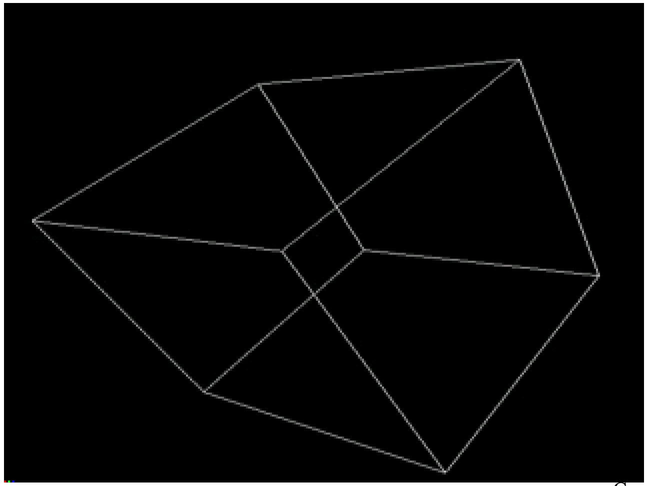

Scalar Field Topology

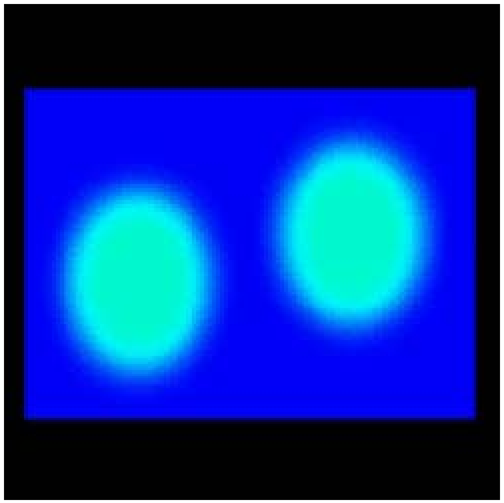

Pion Collision Simulation

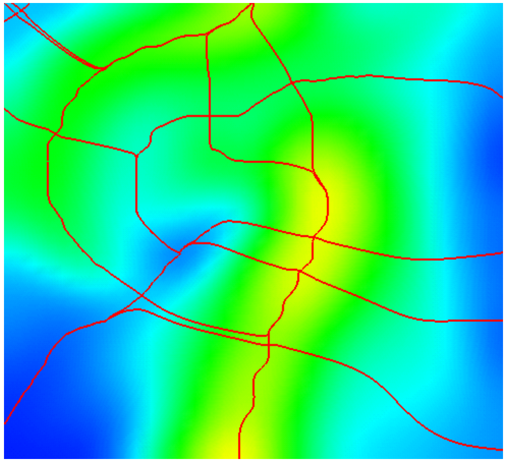

Topology of wind speed in a climate model simulation

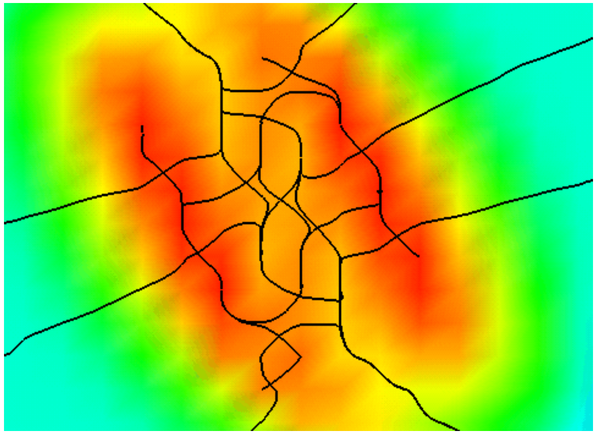

Close-up snapshot of above

Topology of a mathematical function reveals information hidden in contour display

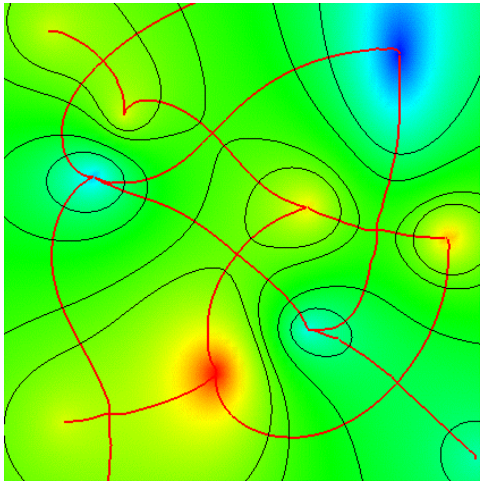

3D Scalar Field

$f(x, y, z)$

Critical Points ⟷ $\nabla f = \begin{pmatrix} f_x \\ f_y \\ f_z \end{pmatrix} = 0$

First Order Local Analysis at the Critical Points ⟷ **Eigenstructure of**

$$H_f = \begin{bmatrix} f_{xx} & f_{xy} & f_{xz} \\ f_{yx} & f_{yy} & f_{yz} \\ f_{zx} & f_{zy} & f_{zz} \end{bmatrix}$$

Critical Points with Linking Curves

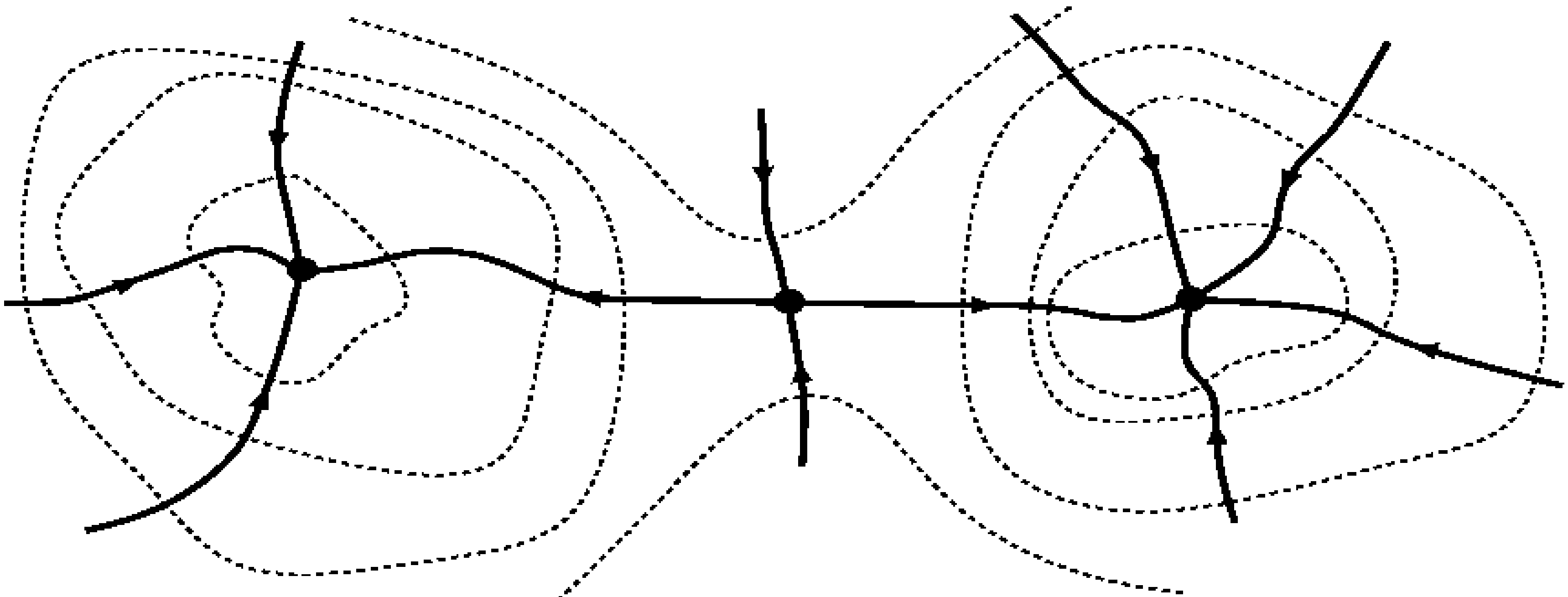

Integral Curves of Vector Field

Solution of ODE : $\vec{U}(\vec{X}) = \dfrac{d\vec{X}}{dt}$ Runge-Kutte, 4th Order Integration

Single Stream Functions for 2D incompressible flow (Lagrange1781)

$$p\vec{U} = \frac{\partial \Psi}{\partial x}$$
$$p\vec{U} = \frac{\partial \Psi}{\partial y}$$

for integral curves

$$\partial \Psi = 0$$

Dual Stream Functions for Solenoidal Vector Fields (zero divergence) [Yih1957]

$$p\vec{U} = \nabla f \times \nabla g$$

and obey law of mass conservation

Ref: Dual Stream Functions, David Kenwright's Thesis1993, Auckland
Also: Bajaj, Xu, Spline Approx. of Algebraic Surface-Surface Intersection Curves, Advances in Comp. Math, 1996

Topology preserving, Finite Element Interpolants

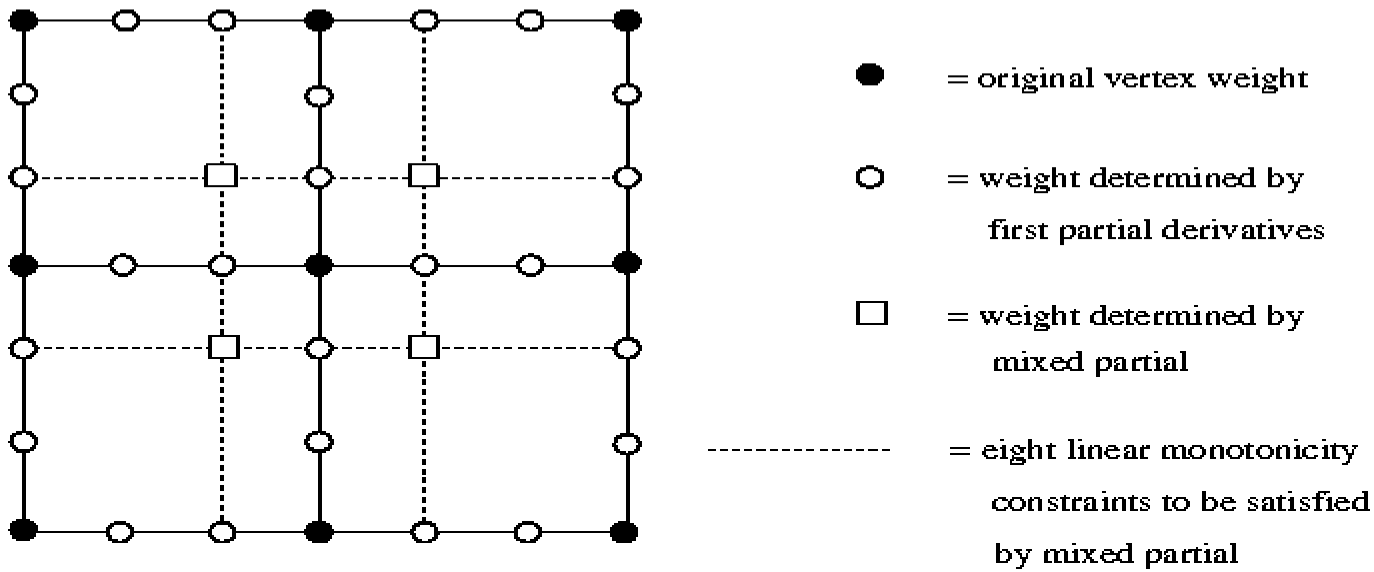

Open question:

What is the true interpolant which does not perturb the topology of the underlying data ?

Vector Topology in 3D:

Topology Preserving Interpolation

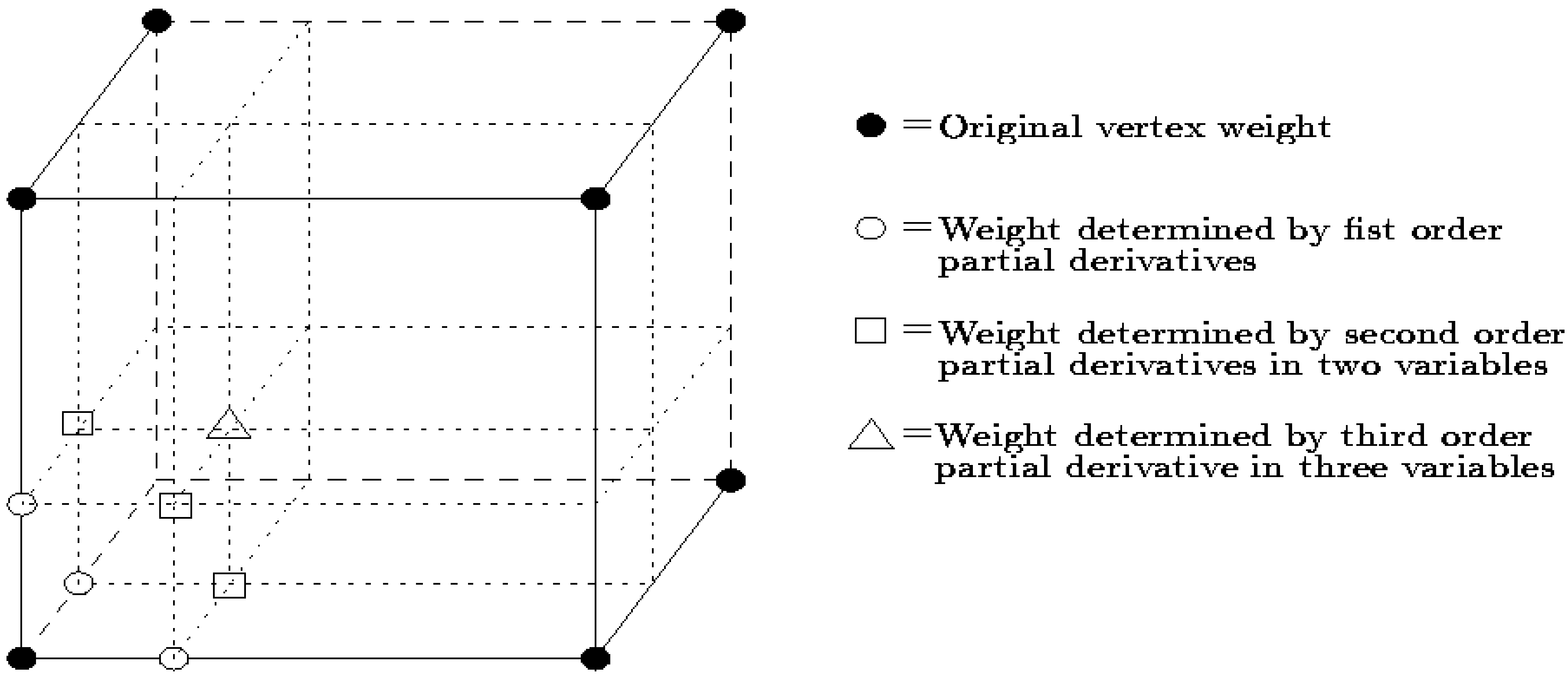

Open Questions : Field Topology preservation ?

Scalar Topology (3D structure enhancement)

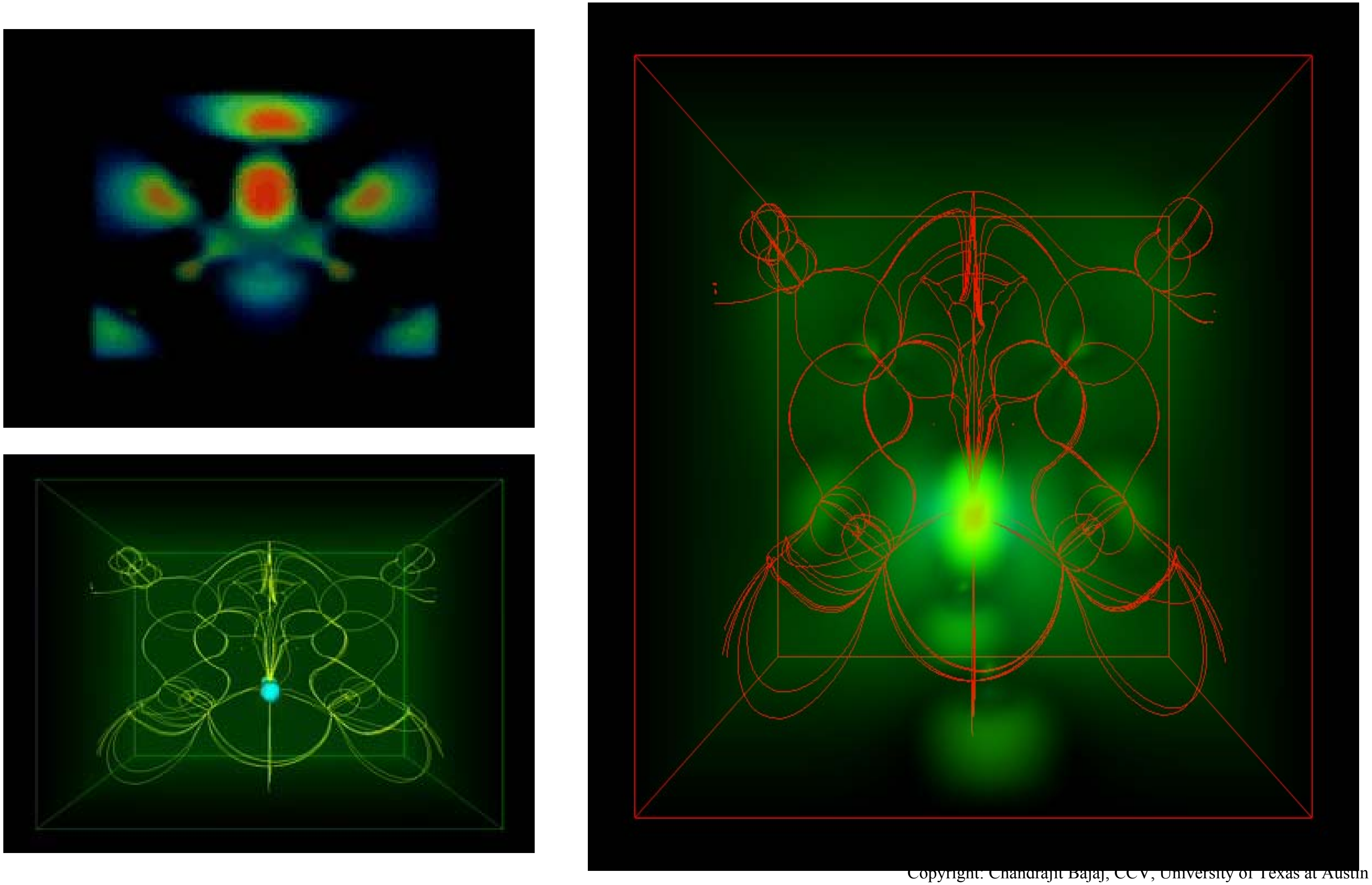

Scalar Topology
(Road Map for Data Exploration)

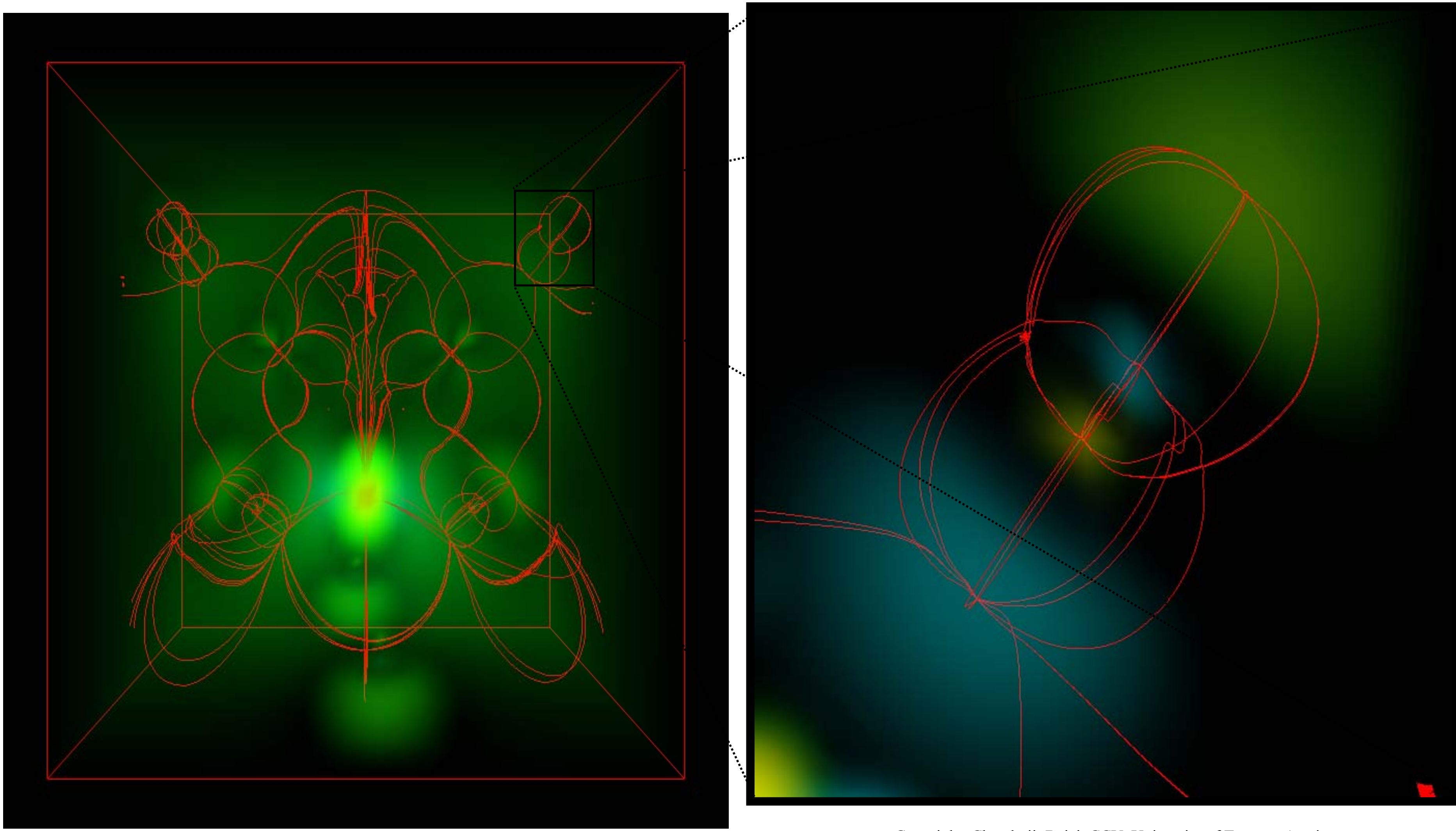

Scalar Topology

dynamic structure tracking

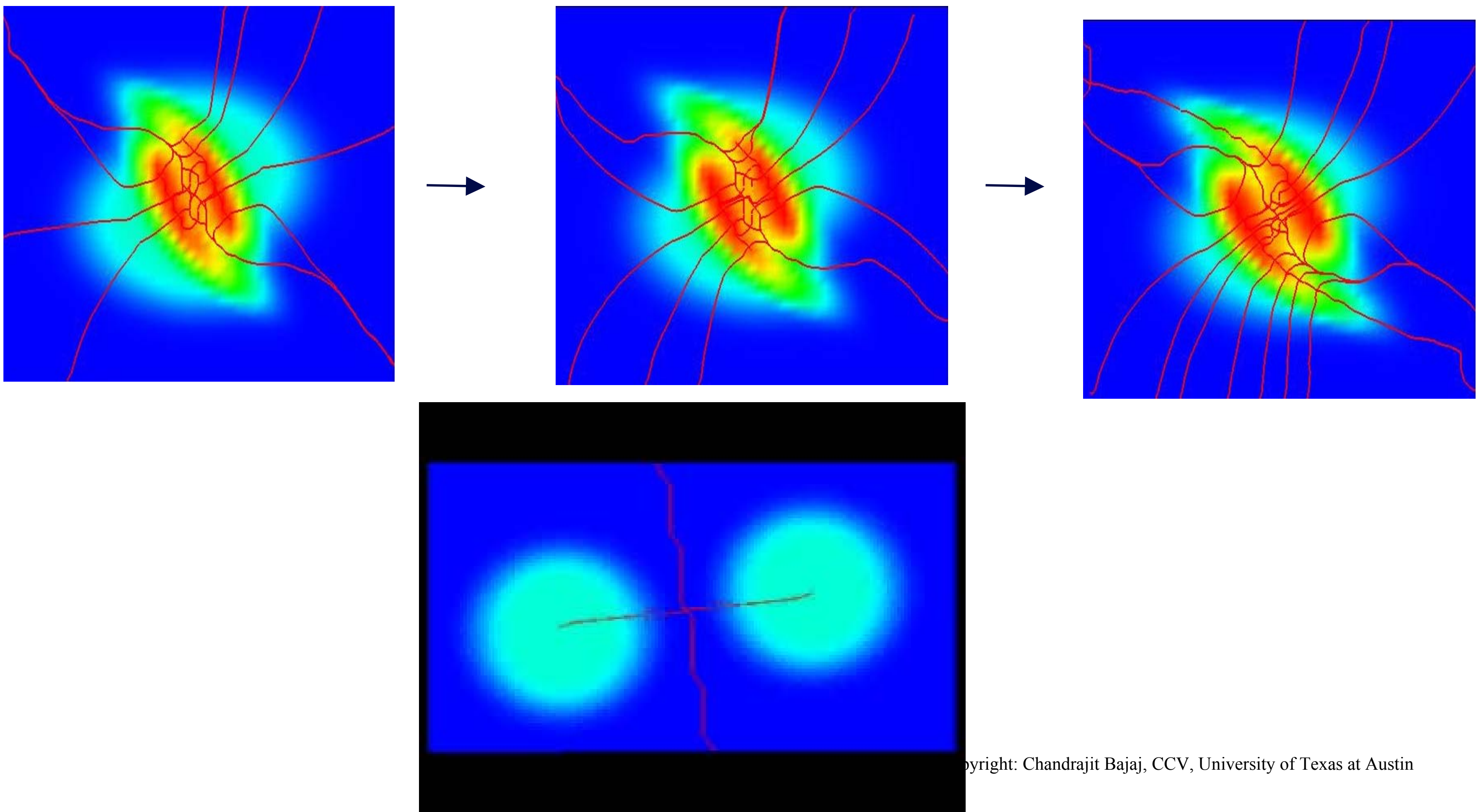

Feature Preserving Decimation of Pion Collision

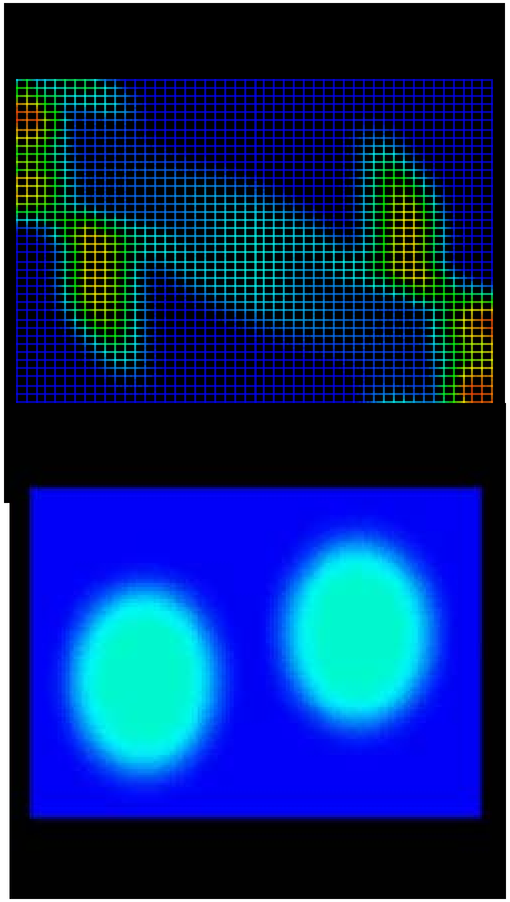

51-timestep simulation of a Pion Collision (Original 12 data variables over a rectilinear mesh)

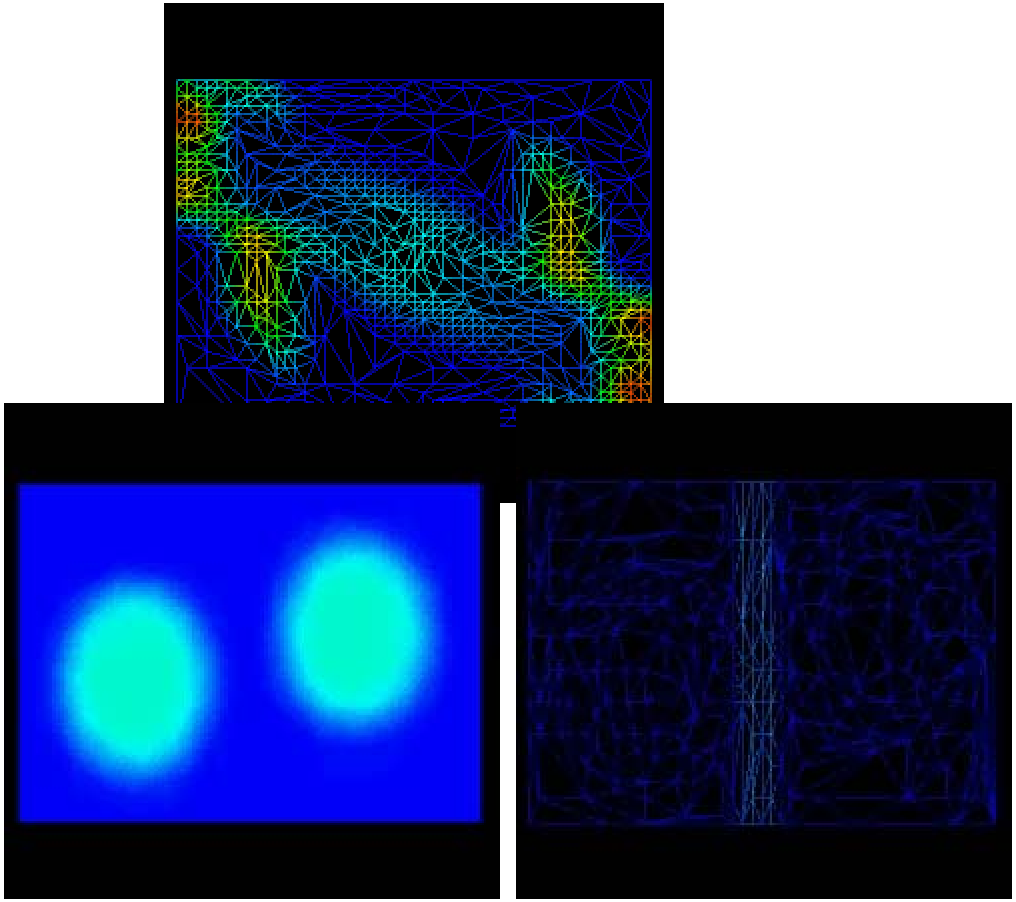

Pion Collison after 3% error-bounded decimation (all variables) of 60% -85% per timestep

Topology Preserving Simplification (J. of Computers & Graphics, 1998)

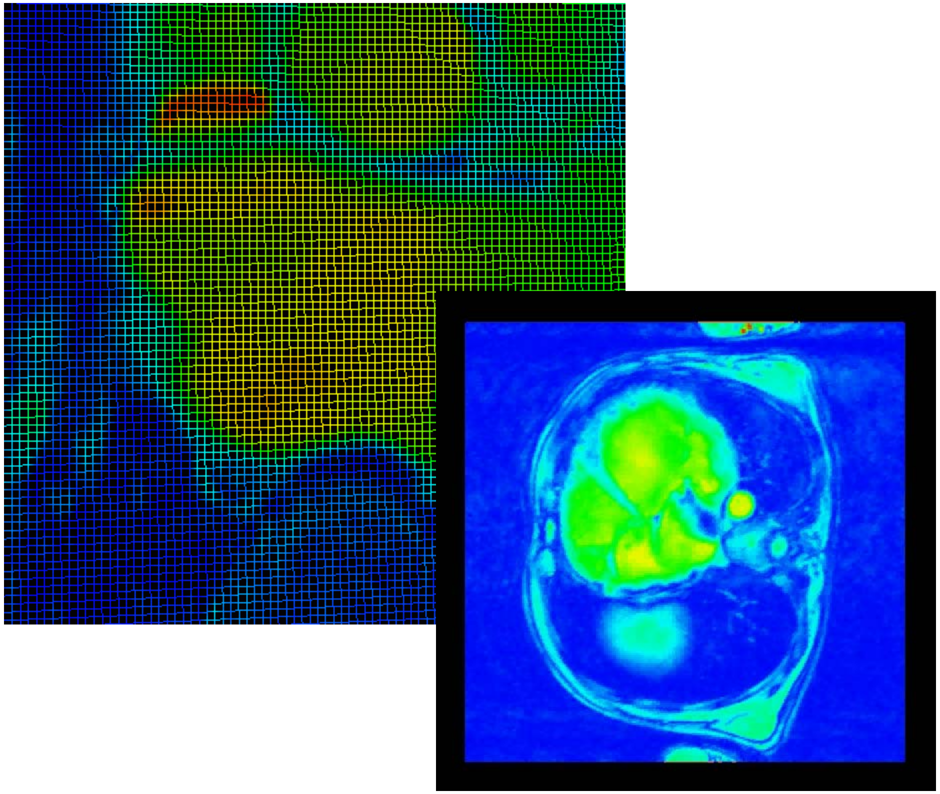

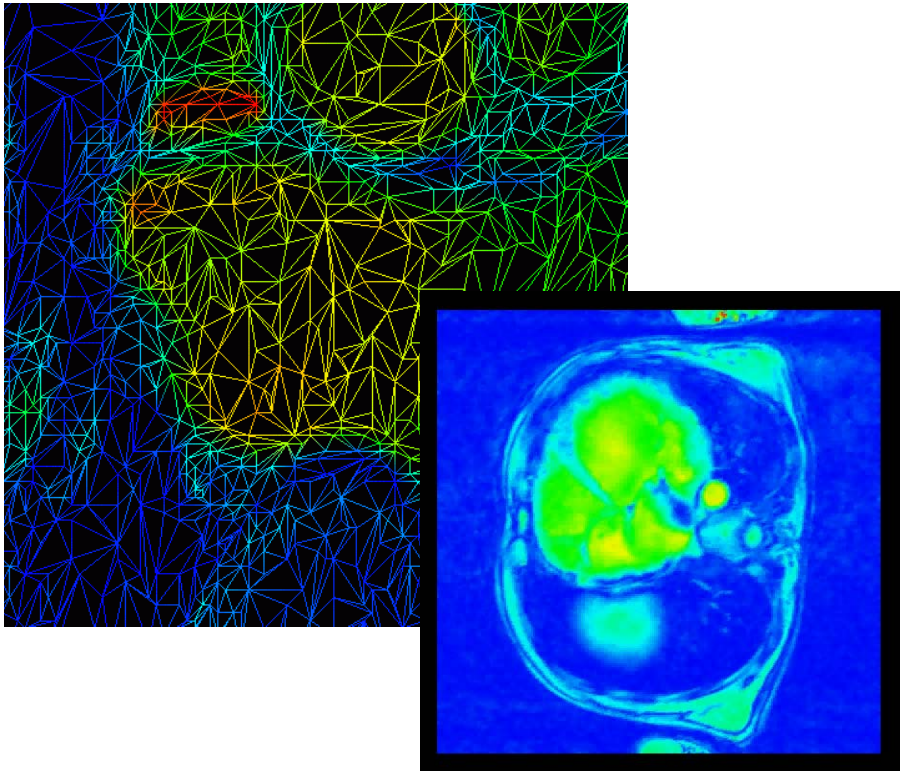

Original Data (130050 tri)

7% Error
(90% reduced, 13061 tri)

Data Courtesy Tsuyoshi Yamamoto and Hiroyuki Fukuda, Hokkaido University

Gated MRI Closeup

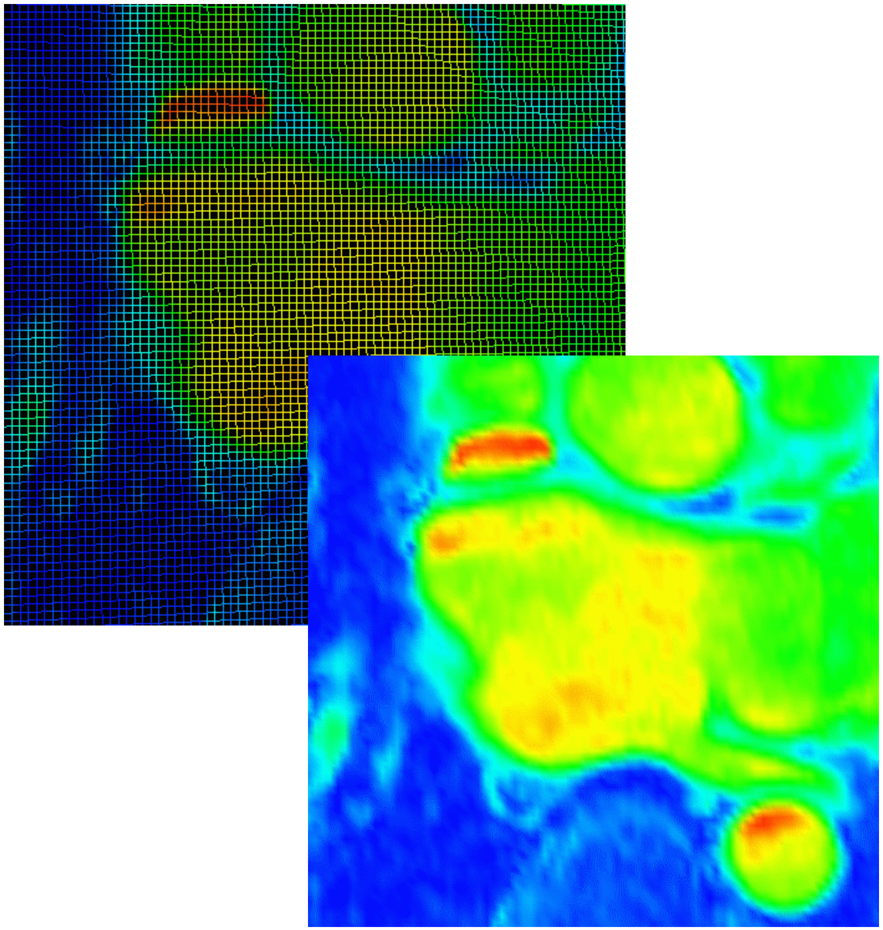

Original Data (130050 tri)

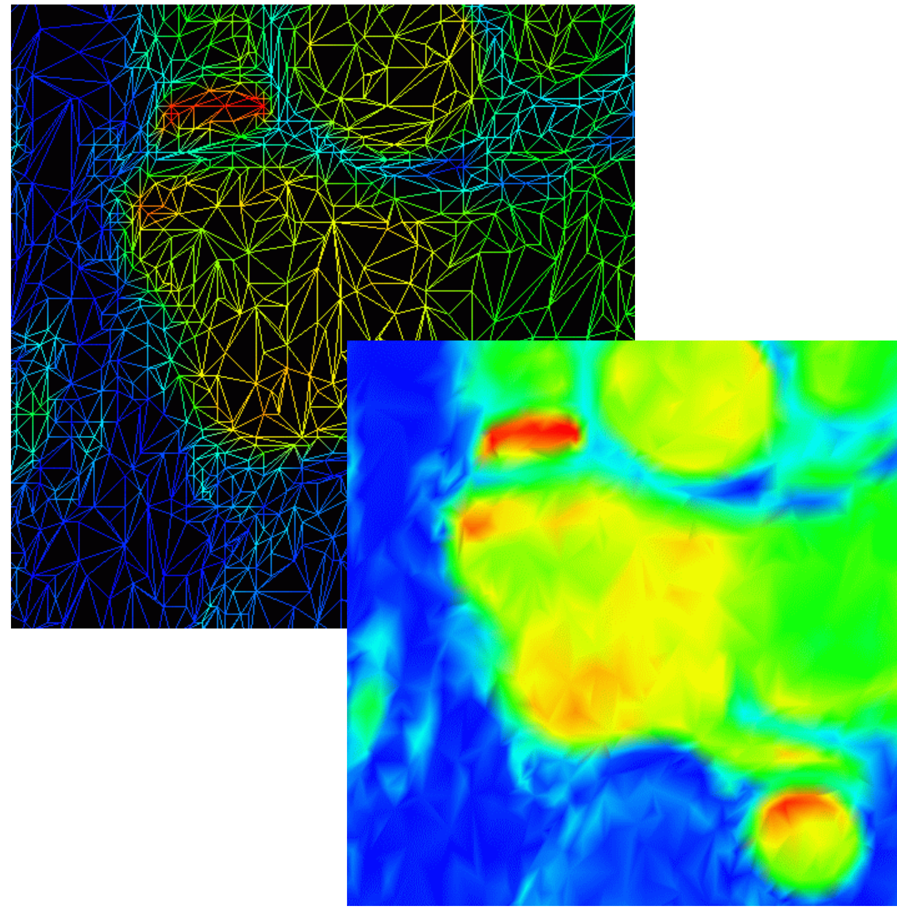

7% Error
(90% reduced, 13061 tri)

To wake up with coffee!
Or Mineralwasser !!

Curves $f(x,y) = 0$, 2D Scalar Fields

- I Critical Points are Singularities
- nodal, cuspidal, tacnodal, higher order
- II Classification of singularities
- simple: eigenvalues of Hessian of f
- higher order: Weierstrass preparation followed by
- a Newton factorization both using bivariate Hensel Lifting
- Ref: Abhyankar, Bajaj, Rational Parameteriz. Of Algebraic Curves, CAGD
- Bajaj, Xu, *Rational Spline Approx. of Plane Algebraic Curves*, J of Comp. Math, 1995,

Weierstrass, Newton and Pade'

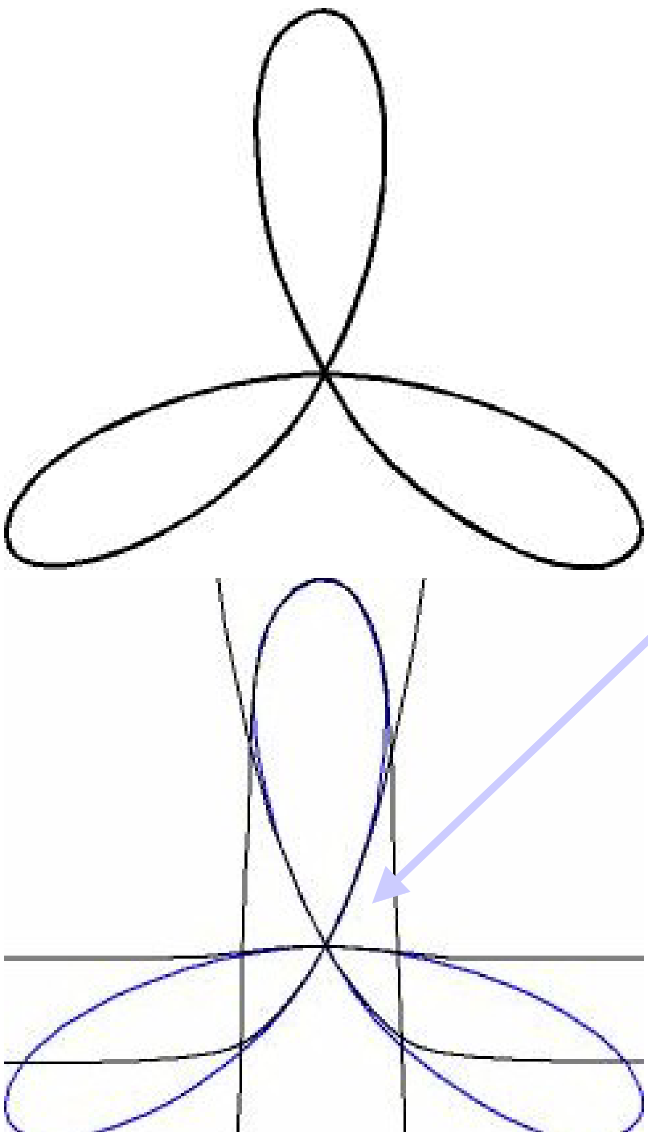

Weierstrass (x^3-x^2+y^2,6)

•••

Newton ((x^2+y^2)^2+3*x^2*y-y^3,0,4)

•••

localpower2d (x^3-x^2+_y^2,s,6,0,0)

•••

Global Parameterization of Real Algebraic Curves

- Computation of Real Curve Genus

- Real Rational Parameterization of Real Curves of Genus 0

Ref:

- Abhyankar, Bajaj, Computer Aided Design 1987
- Recio, Sendra, Winkler

  J. of Symbolic Computation, 1995, 1997

Piecewise Rational Parameterizations of Real Algebraic Curves

Problem

Given a real algebraic plane curve **C**: $f(x, y) = 0$ of degree d and of arbitrary genus, a box ***B*** defined by $\{(x, y) | \alpha \le x \le \beta, \gamma \le y \le \delta\}$, an error bound $\varepsilon > 0$, and integers *m,n* with $m + n \le d$ construct a C^0 or C^1 continuous piecewise rational ε-approximation of all portions of **C** within the given bounding box **B**, with each rational function $\frac{P_i}{Q_i}$ of degree $P_i \le m$ and degree $Q_i \le n$.

Sketch of Algorithm

1. Compute all intersections of **C** within the given bounding box ***B*** and also the tracing direction at these points. Next, compute all singular points *S* and *x*-extreme points *T* in the bounded plane curve $\mathbf{C_B}$.

2. Compute a Newton factorization for each singular point (x_i, y_i) in ***S*** and obtain a power series representation for each analytic branch of **C** at (x_i, y_i) and given by

$$\begin{cases} X(s) = x_i + s^{k_i} \\ Y(S) = \sum_{j=0}^{\infty} c_j^{(i)} s^j, \qquad c_0^{(i)} = y_i \end{cases} \qquad (2.1)$$

or

$$\begin{cases} Y(s) = y_i + s^{k_i} \\ X(s) = \sum_{j=0}^{\infty} \tilde{c}_j^{(i)} s^j, \qquad \tilde{c}_0^{(i)} = x_i \end{cases} \qquad (2.2)$$

Sketch of Algorithm (contd)

3. Without loss of generality, consider the case where the analytic branch at the singularity is of type (2.1). Compute $\frac{P_{mn}(s)}{Q_{mn}(s)}$ the (m,n) Padé approximation of Y(s). That is

$$\frac{P_{mn}(s)}{Q_{mn}(s)} - Y(s) = O(s^{m+n+1})$$

4. Compute $\beta > 0$ a real number, corresponding to points $(\tilde{x}_i = X(\beta), \tilde{y}_i = Y(\beta))$ and $(\hat{x}_i = X(-\beta), \hat{y}_i = Y(-\beta))$ on the analytic branch of the original curve **C**, such that $\frac{P_{mn}(s)}{Q_{mn}(s)}$ is convergent for $s \in [-\beta, \beta]$

Sketch of Algorithm (contd)

5. Modify $P_{mn}(s)/Q_{mn}(s)$ to $\widetilde{P}_{mn}(s)/\widetilde{Q}_{mn}(s)$ is C^1 continuous approximation of $Y(s)$ on $[0, \beta]$

6. Denote the set of all the points $(\widetilde{x}_{i,}\widetilde{y}_i),(\hat{x}_{i,}\hat{y}_i),$ the set T and the boundary points of $\mathbf{C}_B$ by V. The curve $\mathbf{C}_B$ yields a natural graph G having V, as its vertex set and the set of curve segments of $\mathbf{C}_B$ joining any pair of points in V, as its edge set E. Now starting from each (simple) point $(x_{i,}y_i)$ in V we trace out the graph G, approximating each of its edges E by C^1 continuous piecewise rational curves.

Piecewise Rational Parameterization Approximations for decreasing error

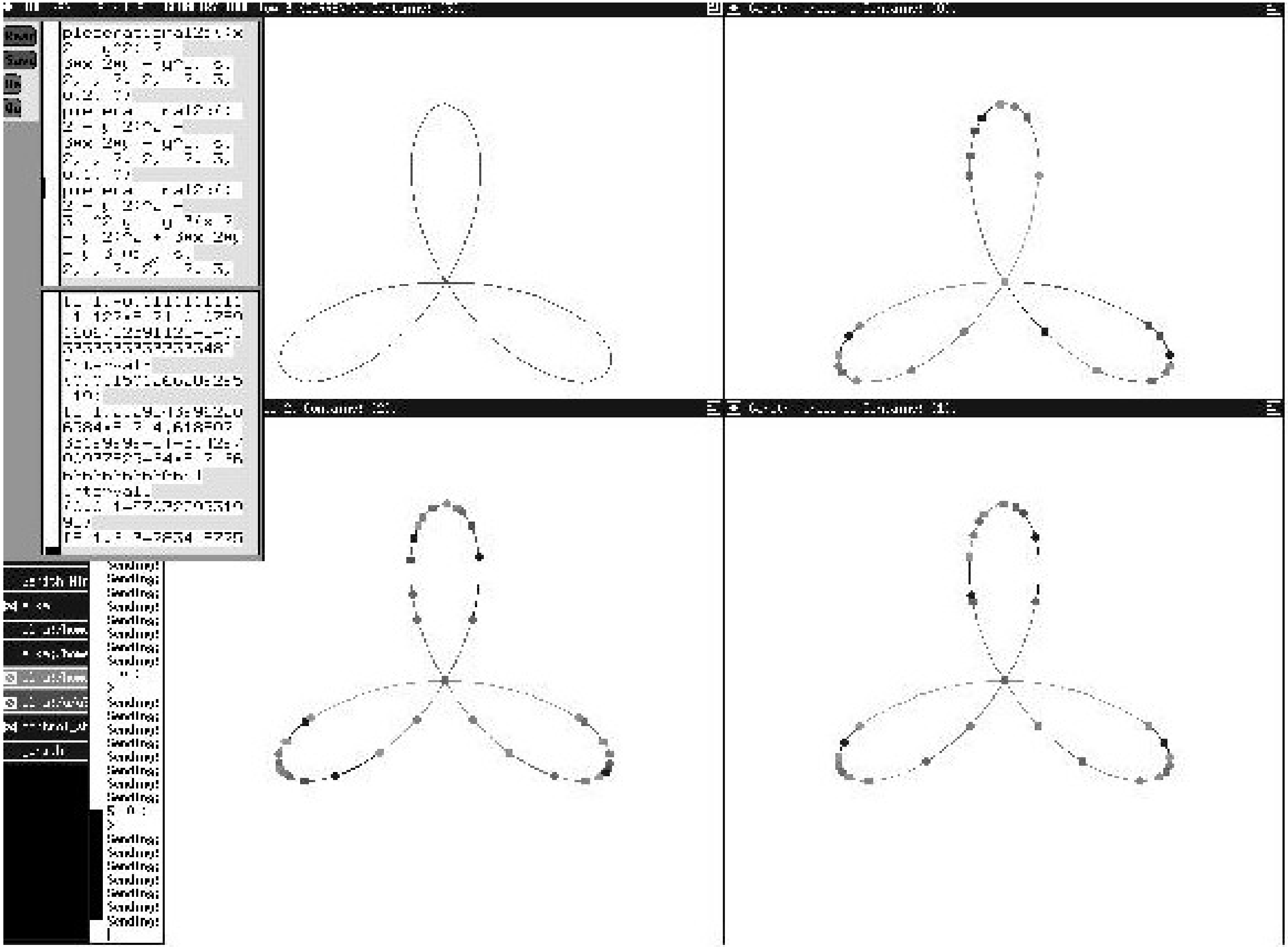

Expansion at Singular Points

Hensel Lifting

Consider $f(x, y)$ of degree d and monic in y

$$f(x,y) = f_0(y) + f_1(y)x + \cdots + f_k(y)x^k + \cdots$$

We wish to compute real power series factors *g(x,y)* and *h(x,y)* = g(x,y)h(x,y)
The technique of Hensel lifting allows one to reconstruct the power series factors

$$g(x,y) = g_0(y) + g_1(y)x + \cdots + g_i(y)x^i + \cdots$$

$$h(x,y) = h_0(y) + h_1(y)x + \cdots + h_j(y)x^j + \cdots$$

From initial factors $f(0,y) = f_0(y) = g_0(y)h_0(y)$

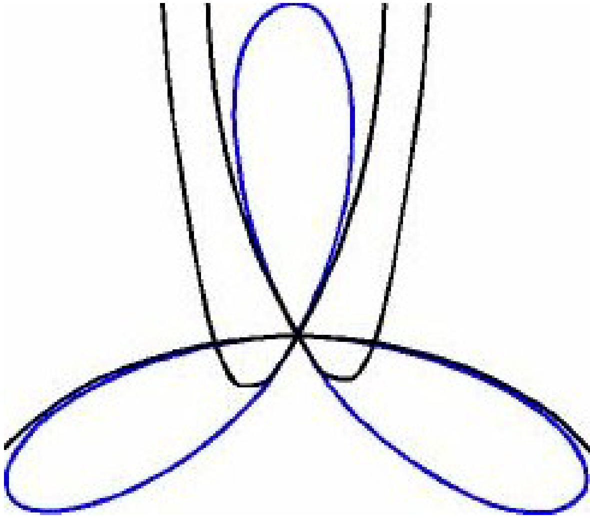

Weierstrass Factorization

A Weierstrass power series factorization is of the form

$$f(x,y) = g(x,y)\underbrace{(y^e + a_{e-1}(x)y^{e-1} + \cdots + a_0(x))}_{h(x,y)}$$

Where g(x,y) is a unit power series

The Weierstrass preparation can be achieved via Hensel Lifting from the initial factors:

$$f(0,y) = f_0(y) = \underbrace{(a_0 + a_1 y + \cdots)}_{g_0(y)}\underbrace{y^e}_{h_{0(y)}},$$

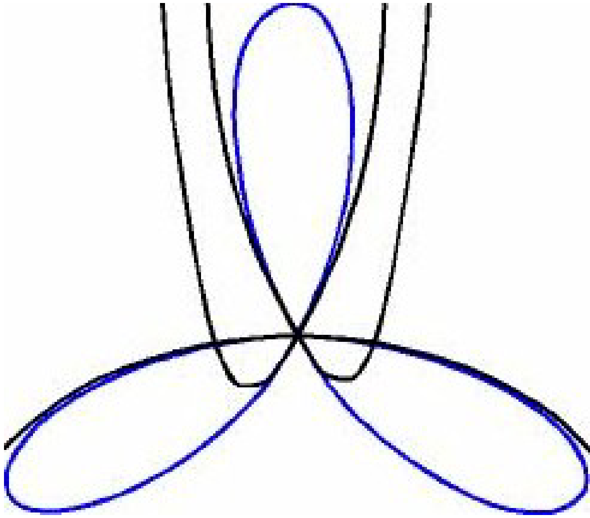

Newton Factorization

Let

$$h(x,y) = y^e + a_{e-1}(x)y^{e-1} + \cdots + a_0(x)$$

Then it is possible to factor h(x,y) into real linear factors of the type using Hensel Lifting

$$h(x,y) = \prod_{i=1}^{e}(y - \eta_i((t)))$$

Surfaces $f(x,y,z) = 0$, 3D Scalar Fields

- I Critical Points (& Curves) are Singularities
- points: difficult ?
- curves: nodal, cuspidal, tacnodal, higher order
- II Classification of singularities
- simple points: eigenvalues of Hessian of f
- higher order points : ??
- Curves : some similar to singular points on curves. Others ?

- *Ref: Bajaj, Xu, Rational Spline Approx. of Real Algebraic Surfaces, J of Symbolic Computation, 1997*

Topology Preserving Spline Approximations and Display of Real Algebraic Surfaces

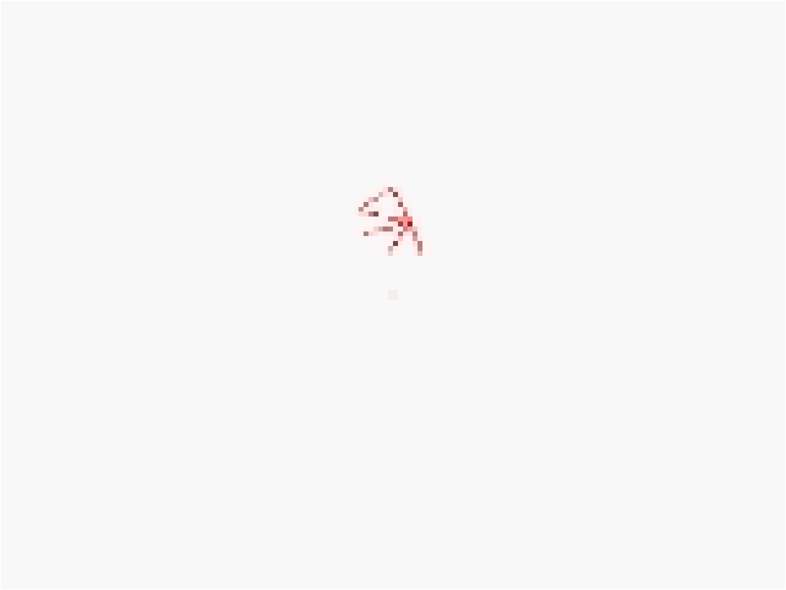

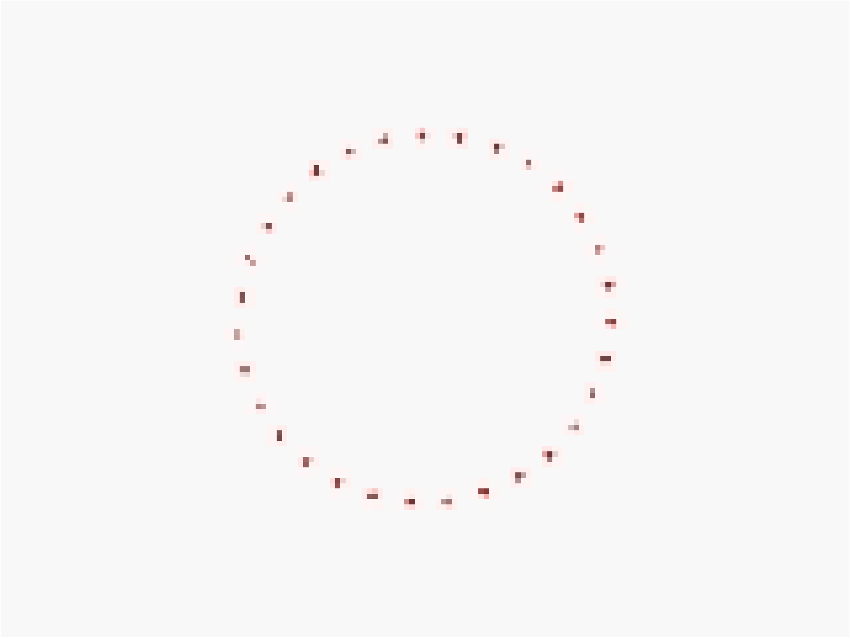

Global Rational Parameterization for Real Algebraic Surfaces

- Computation of Arithmetic Genus, Second Plurigenus
- Parametrization of Real Surfaces satisfying Castelnuovo criterion for rationality ?

- Ref: J. Schicho, Journal of Symbolic Computation 1997

Global Rational Parameterization of Non-Singular Real Cubic Surfaces

Given two skew lines $l_1(u) = \begin{bmatrix} x_1(u) \\ y_1(u) \\ z_1(u) \end{bmatrix}$ and $l_2(v) = \begin{bmatrix} x_2(v) \\ y_2(v) \\ z_2(v) \end{bmatrix}$

On the cubic surface $f(x, y, z) = 0$, the cubic rational parametrization formula for a point $\mathbf{p}(u, v)$ on the surface is

$$\mathrm{P}(u,v) = \begin{bmatrix} x(u,v) \\ y(u,v) \\ z(u,v) \end{bmatrix} = \frac{a l_1 + b l_2}{a+b} = \frac{a(u,v) l_1(u) + b(u,v) l_2(v)}{a(u,v)+b(u,v)}$$

where

$$a = a(u,v) = \nabla f(l_2(v)) \cdot [l_1(u) - l_2(v)]$$

$$b = b(u,v) = \nabla f(l_1(v)) \cdot [l_1(u) - l_2(v)] \cdot$$

Twenty-Seven Lines on a Cubic Surface

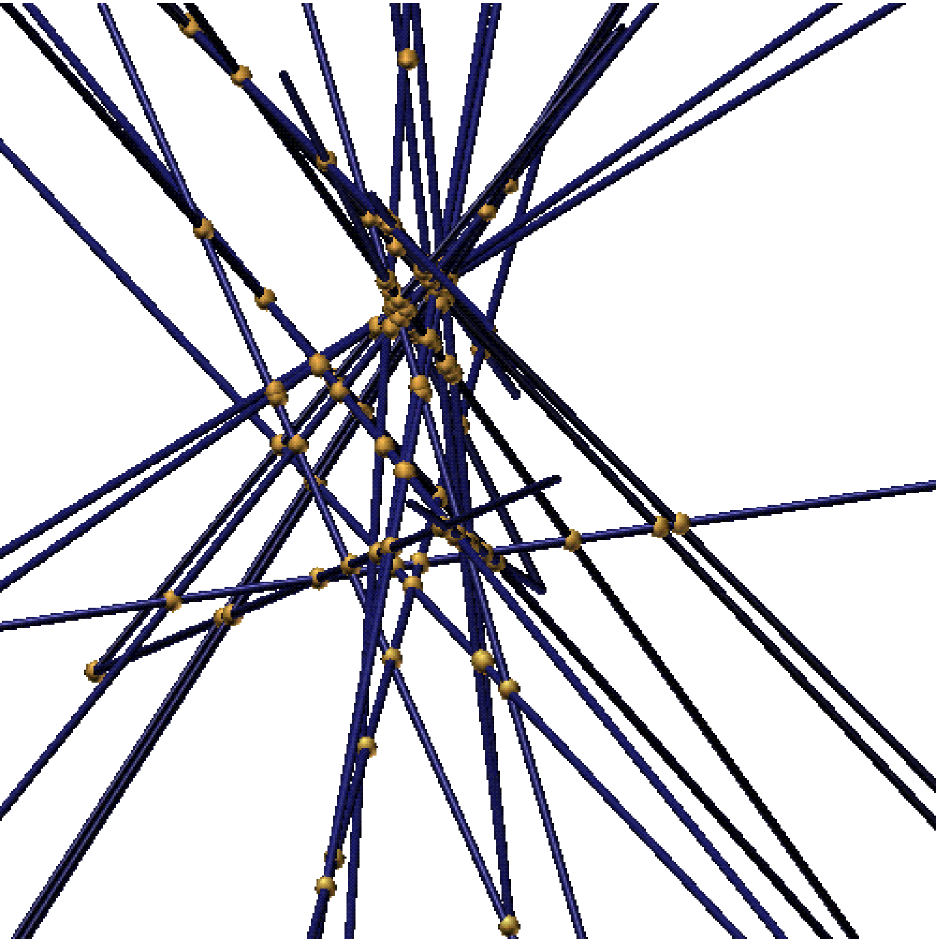

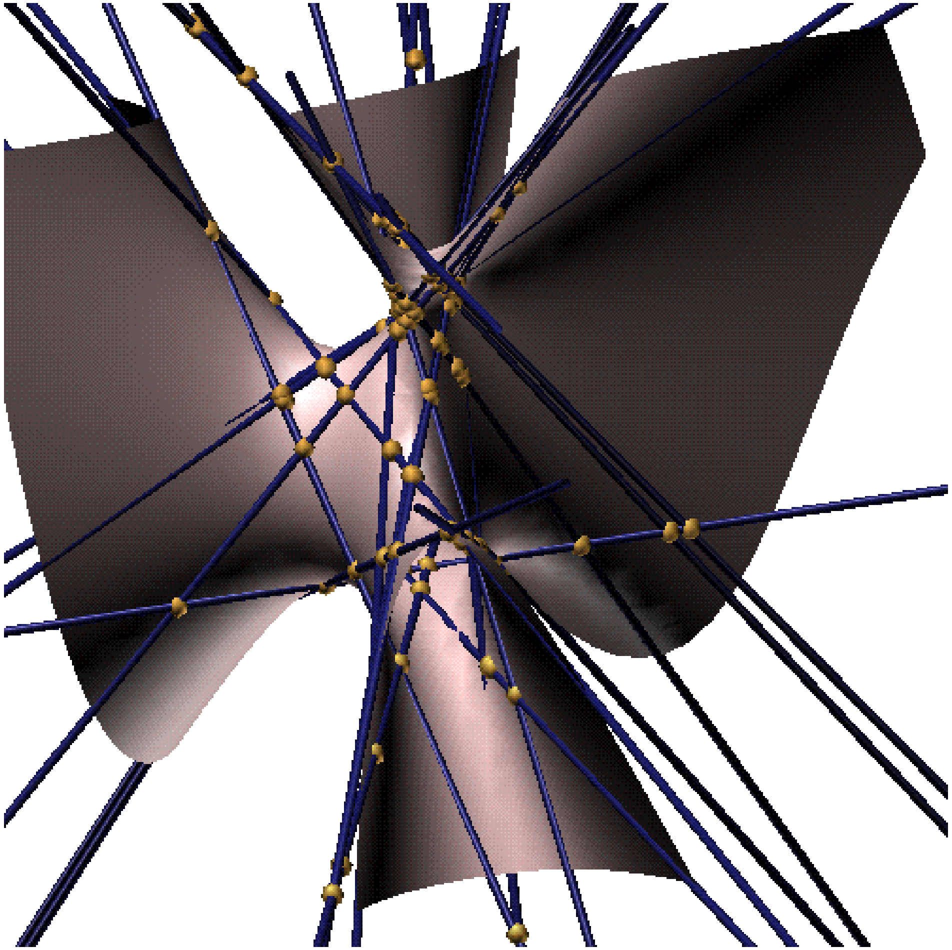

Twenty-Seven Lines on the Cubic Surface
(Schlafi's double-six)

$$\hat{f}_2(\hat{x},\hat{y})+\hat{g}_3(\hat{x},\hat{y})=0$$

THEOREM 1. *The polynomial $P_{81}(t)$ obtained by taking the resultant of* $\hat{f}_2$ *and* $\hat{g}_3$ *factors as* $P_{81}(t)=P_{27}(t)[P_3(t)]^6[P_6(t)]^6$, *where* $P_3(t)=B''t^3+F''t^2+D''t+A''$ is *the denominator of* *$K(t)$ and $L(t)$, and $P_{(6)}(t)$ is the numerator of* $\bar{S}(t)(P_6(t)=\bar{S}(t)[P_3(t)^2])$.

THEOREM 2. *Simple real roots of $P_{27}(t)=0$ correspond to real lines on the surface.*

Rational Parametrization of Cubic A- Patches in BB form

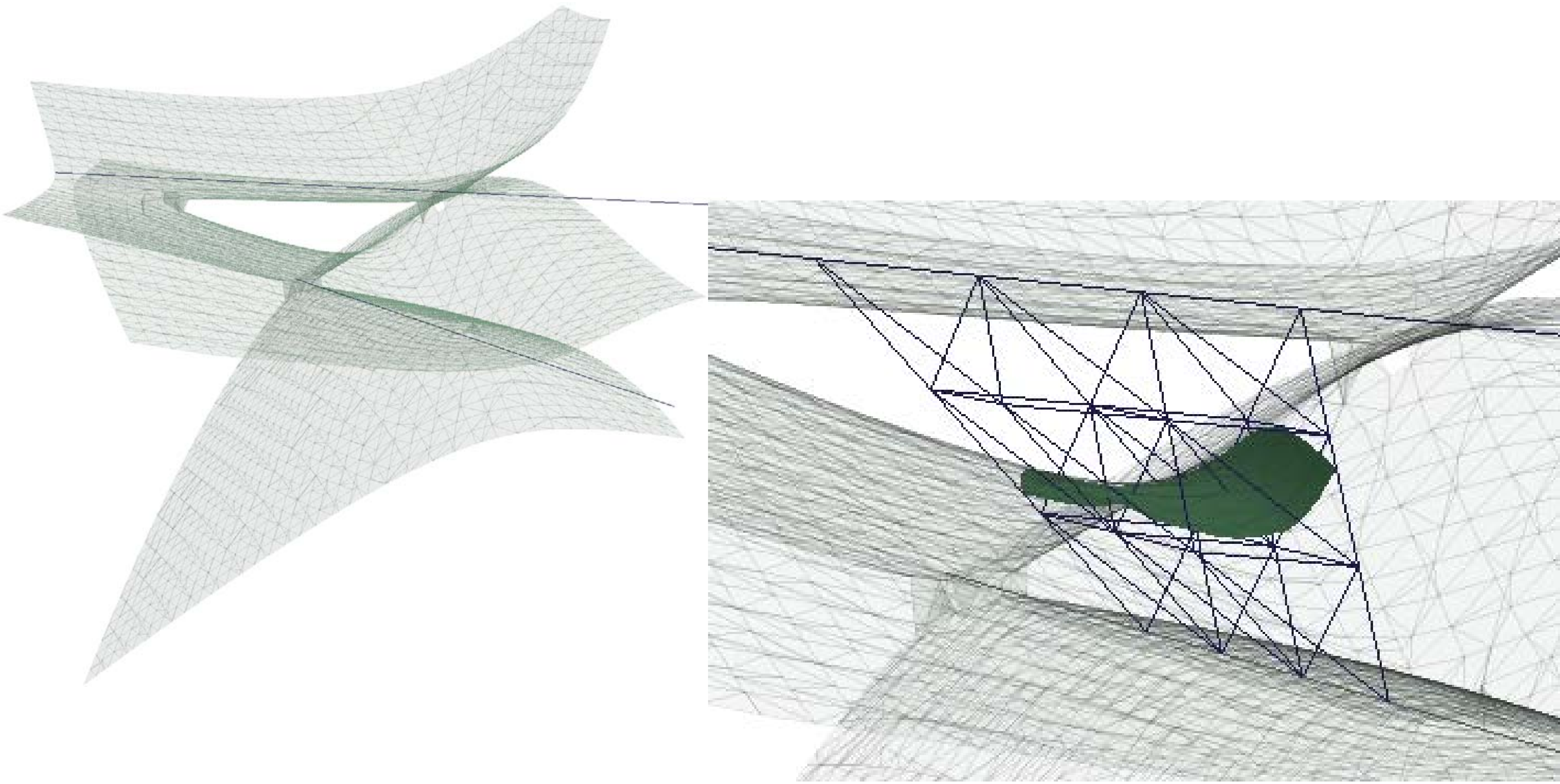

Ref: (ACM Transactions on Graphics'97)

Triangulation and Display of Rational Parametric Surfaces

A rational parametric surface is defined by the three rational functions:

$$x(s,t) = \frac{X(s,t)}{W(s,t)}, \quad y(s,t) = \frac{Y(s,t)}{W(s,t)}, \quad z(s,t) = \frac{Z(s,t)}{W(s,t)}$$

1. **Domain poles**. The map yields a divide by zero at points satisfying $W(s,t) = 0$, the pole of the rational functions. These domain poles are algebraic curves.
2. **Domain base points**. The map is undefined at points satisfying $X(s,t) = Y(s,t) = Z(s,t) = W(s,t) = 0$. There are finitely many such points, called domain *base points*.
3. **Surface singularities**. The given rational surface may be singular.
4. **Complex parameter values**. Some real points of the surface are generated only by complex Parameter values.
5. **Infinite parameter values**. Some finite points of the surface are generated only by infinite parameter values.

Image of a Base Point is a Rational Curve

THEOREM 1 *Let (a,b) be a base point of multiplicity q. Then for any m $\in R$, the image of a domain point approaching (a,b) along a line of slope m is given by (X(m),Y(m),Z(m) W(m) =*

$$\left(\sum_{i=0}^{q}\left(\frac{\partial^q X}{\partial s^{q-i}\partial t^i}(a,b)\right)\binom{q}{i}m^i \cdots \sum_{i=0}^{q}\left(\frac{\partial^q X}{\partial s^{q-i}\partial t^i}(a,b)\right)\binom{q}{i}m^i\right)$$

COROLLARY 1 *If the curves X(s,t) = 0, ...,W(s,t) = 0 share t tangent lines at (a,b), then the seam curve (X(m),Y(m),Z(m),W(m)) has degree q-t. In particular, if X(s,t) = 0 have identical tangents at (a,b), then for all m $\in R$ the coordinates (X(m),...,W(m)) represent a single point.*

Ref: **Bajaj, Royappa** **Triangulation and Display of Arbitrary Rational Surfaces IEEE Visualization Conference 1994**

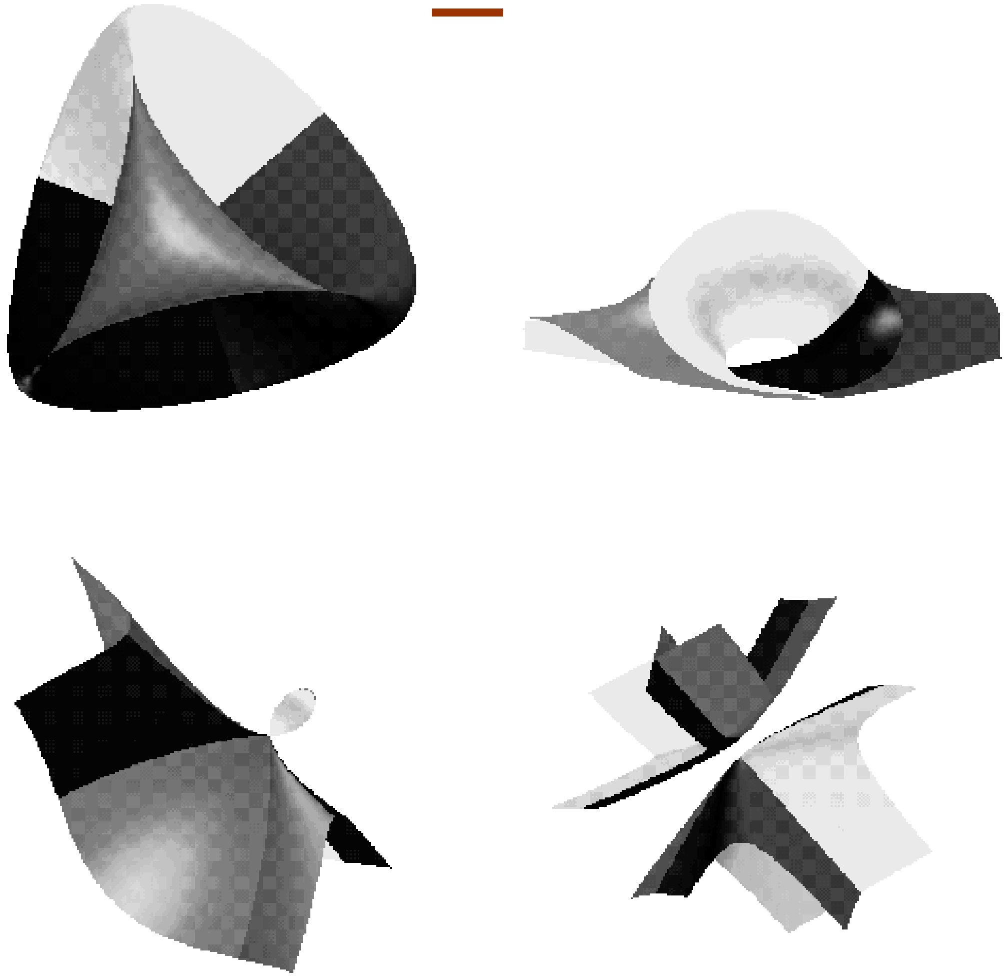

Saddle Points Computation

- Trilinear Interpolant

$$
\begin{aligned}
F(x,y,z) &= F_{000}(1-x)(1-y)(1-z) \\
&+ F_{001}(1-x)(1-y)z \\
&+ F_{010}(1-x)y(1-z) \\
&+ F_{011}(1-x)yz \\
&+ F_{100}x(1-y)(1-z) \\
&+ F_{101}x(1-y)z \\
&+ F_{110}xy(1-z) \\
&+ F_{111}xyz
\end{aligned}
$$

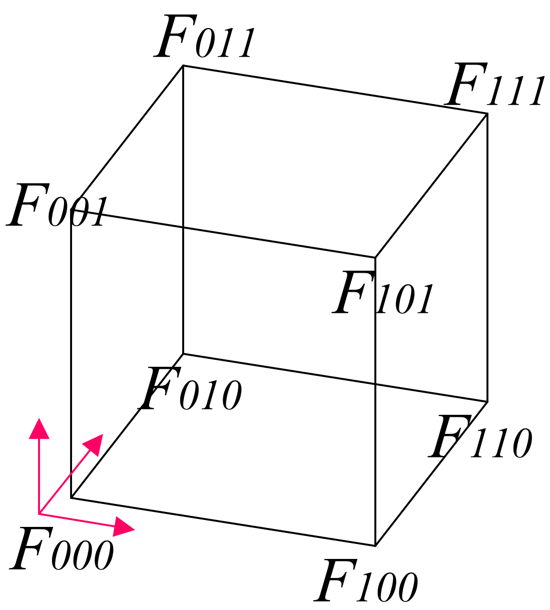

Saddle Points Computation

- Face Saddle Point

  $F(x,y) = ax + by + cxy + d$ (bilinear interpolant)

  First derivatives : $Fx = a + cy = 0$, $Fy = b + cx = 0$

  Saddle point $S = (-b/c , -a/c)$

- Body Saddle Point

  $$F(x,y,z) = a + ex + cy + bz + gxy + fxz + dyz + hxyz$$

  First derivatives = 0 :

  $$F_x = e + gy + fz + hyz = 0$$

  $$F_y = c + gx + dz + hxz = 0$$

  $$F_z = b + fx + dy + hxy = 0$$

Center Computational Visualization CCV

Face and Body Saddle Points

We obtain saddle point :

$$x = -\frac{c+dz}{g+hz}$$

$$y = \frac{k_0+k_1 z}{k_2}$$

$$z = -\frac{g}{h} \pm \frac{\sqrt{g^2k_1^2 - hk_1^{1/2}(ek_2+gk_0)}}{h}$$

$$k_0 = cf - bg, k_1 = df - bh, k_2 = dg - ch$$

Center Computational Visualization CCV

Decision on Topology

- Resolving Face Ambiguity
  - Ambiguity

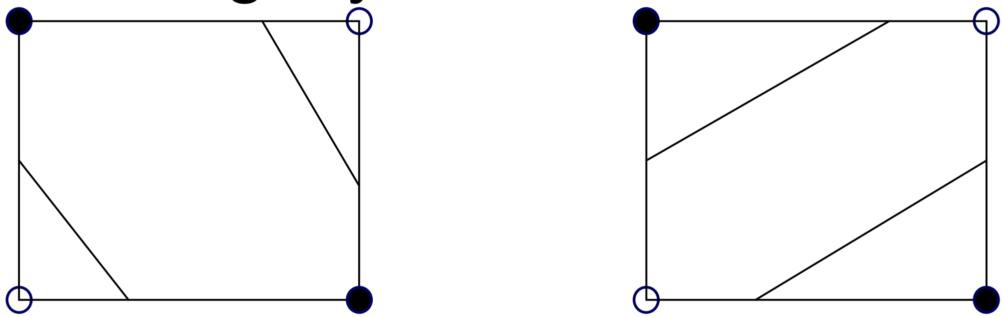

  - Decision based on the value *s* of saddle point

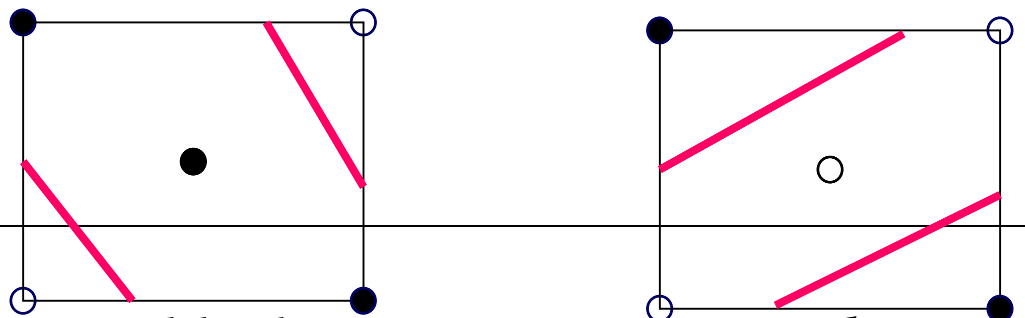

s is black *s is white*

- Resolving Internal Ambiguity
  - Ambiguity

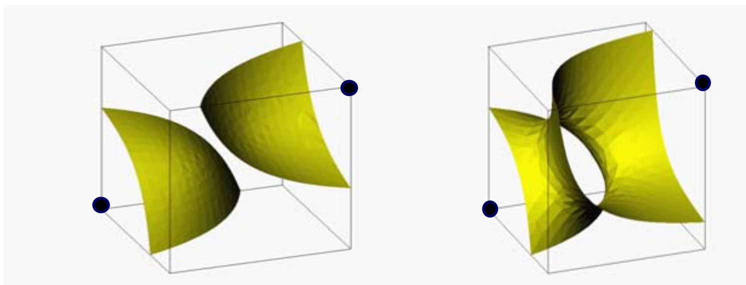

  - Decision based on the value of saddle points

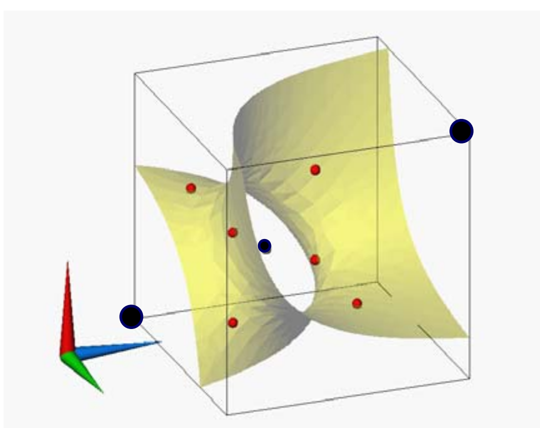

(i) s is black → tunnel

(ii) s is white → two pieces

31 Cases

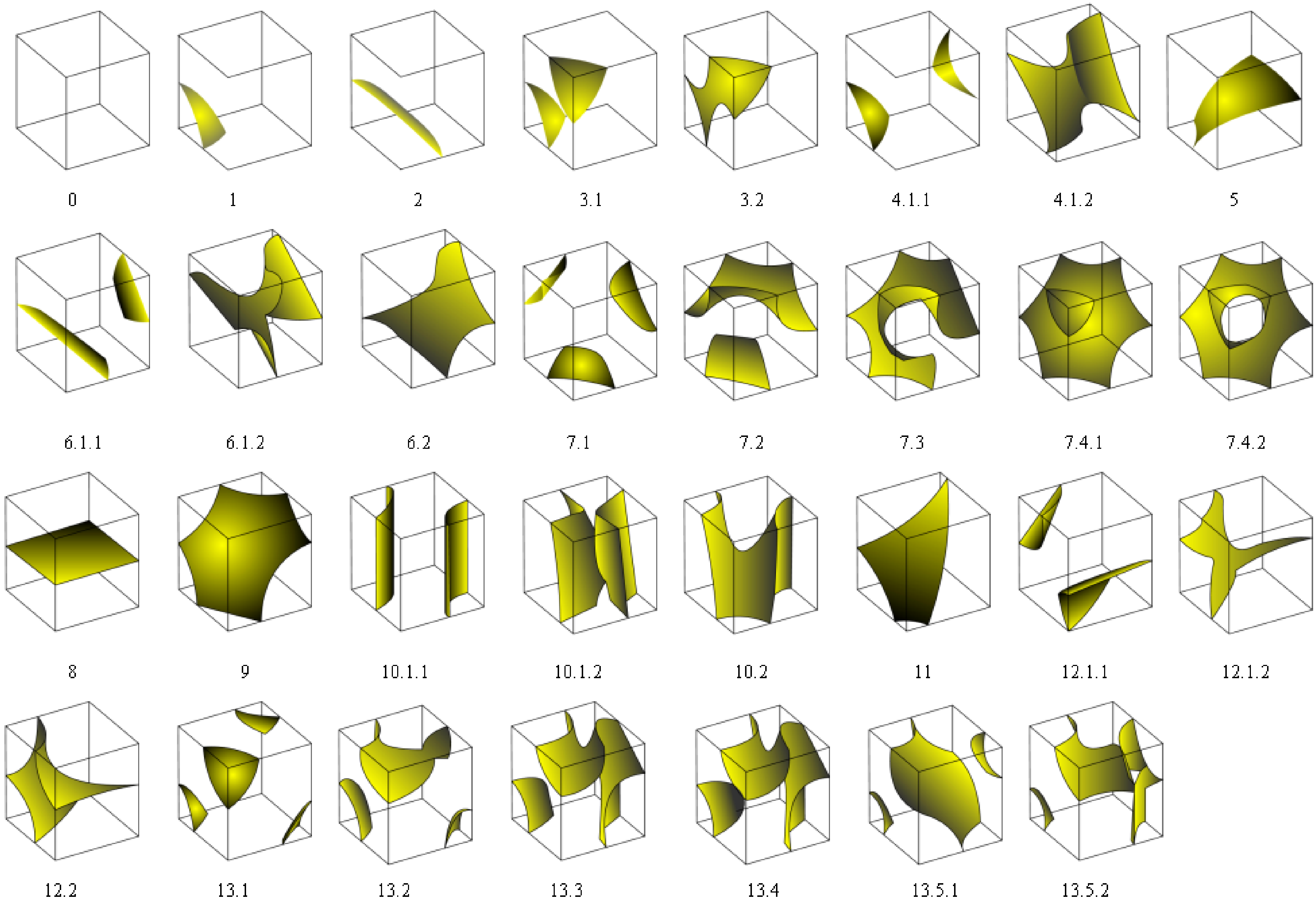
0
1
2
3.1
3.2
4.1.1
4.1.2
5
6.1.1
6.1.2
6.2
7.1
7.2
7.3
7.4.1
7.4.2
8
9
10.1.1
10.1.2
10.2
11
12.1.1
12.1.2
12.2
13.1
13.2
13.3
13.4
13.5.1
13.5.2

Reconstruction from Slices (Bajaj, Klin, J of GMIP'95)

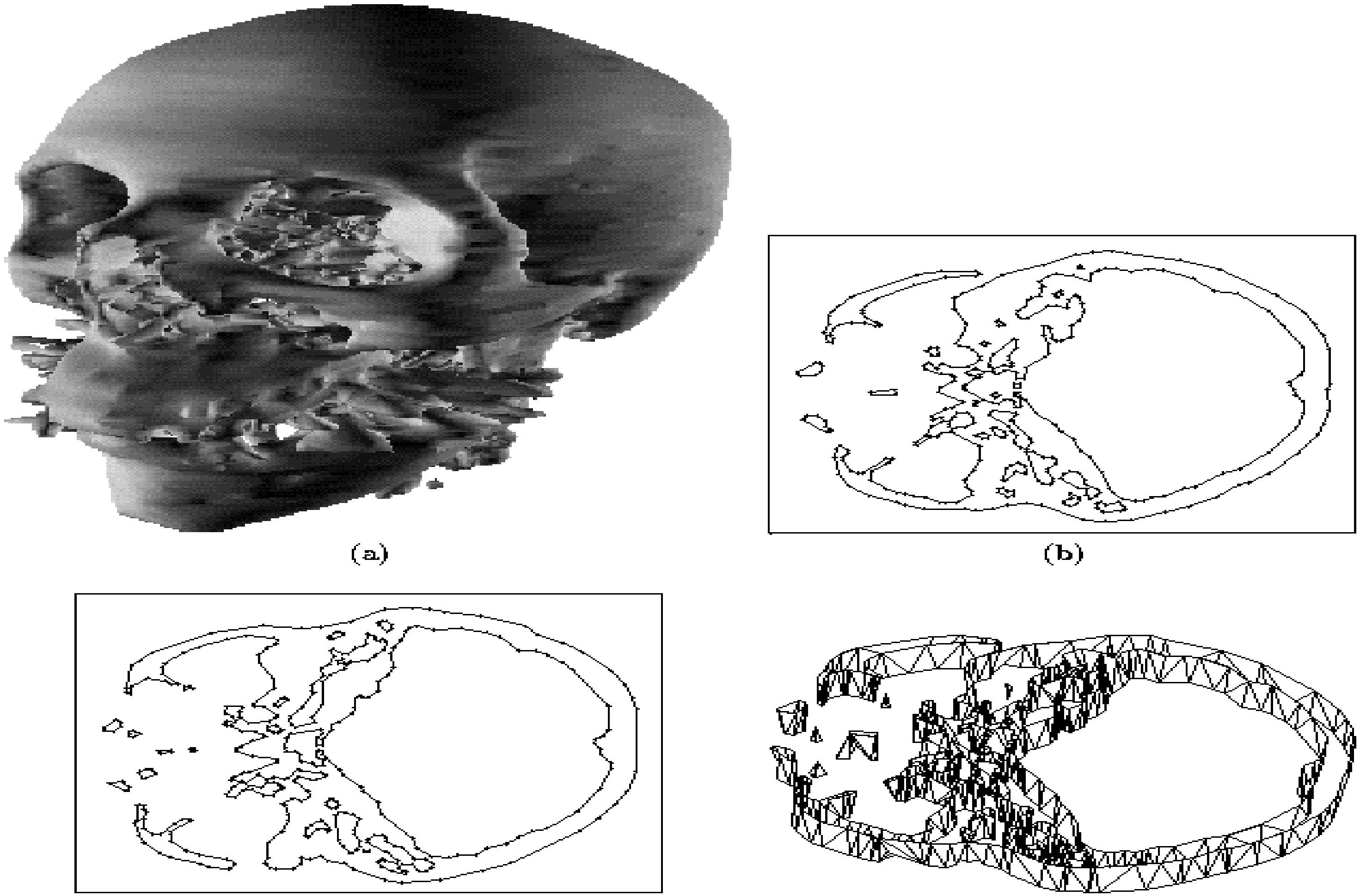

(a) (b) (c) (d)

Topologically correct reconstruction from Volumetric Images

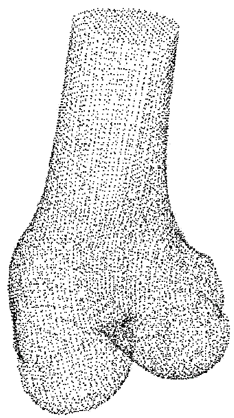

Points cloud

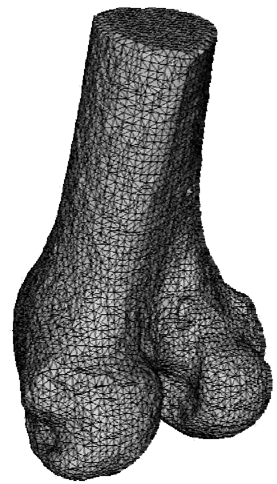

Alpha-Solid

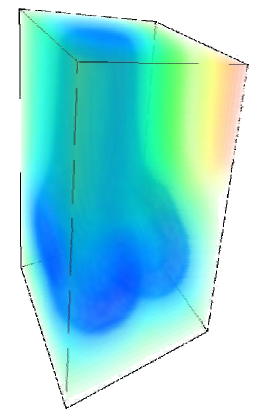

Signed Distance

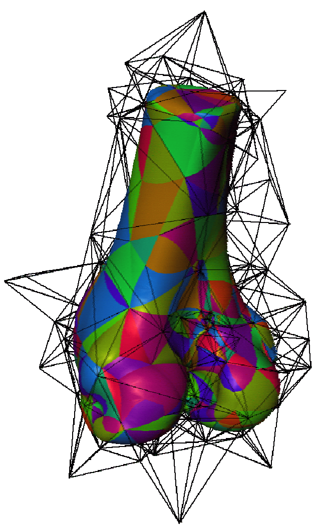

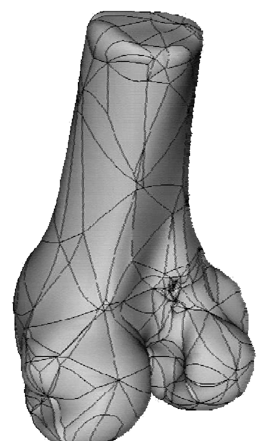

A-Patch BEM

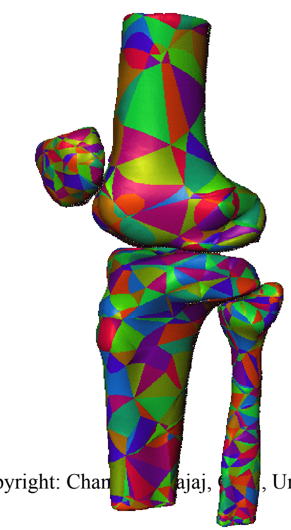

Knee Joint

Use of weights for multiresolution samplings(Siggraph'95)

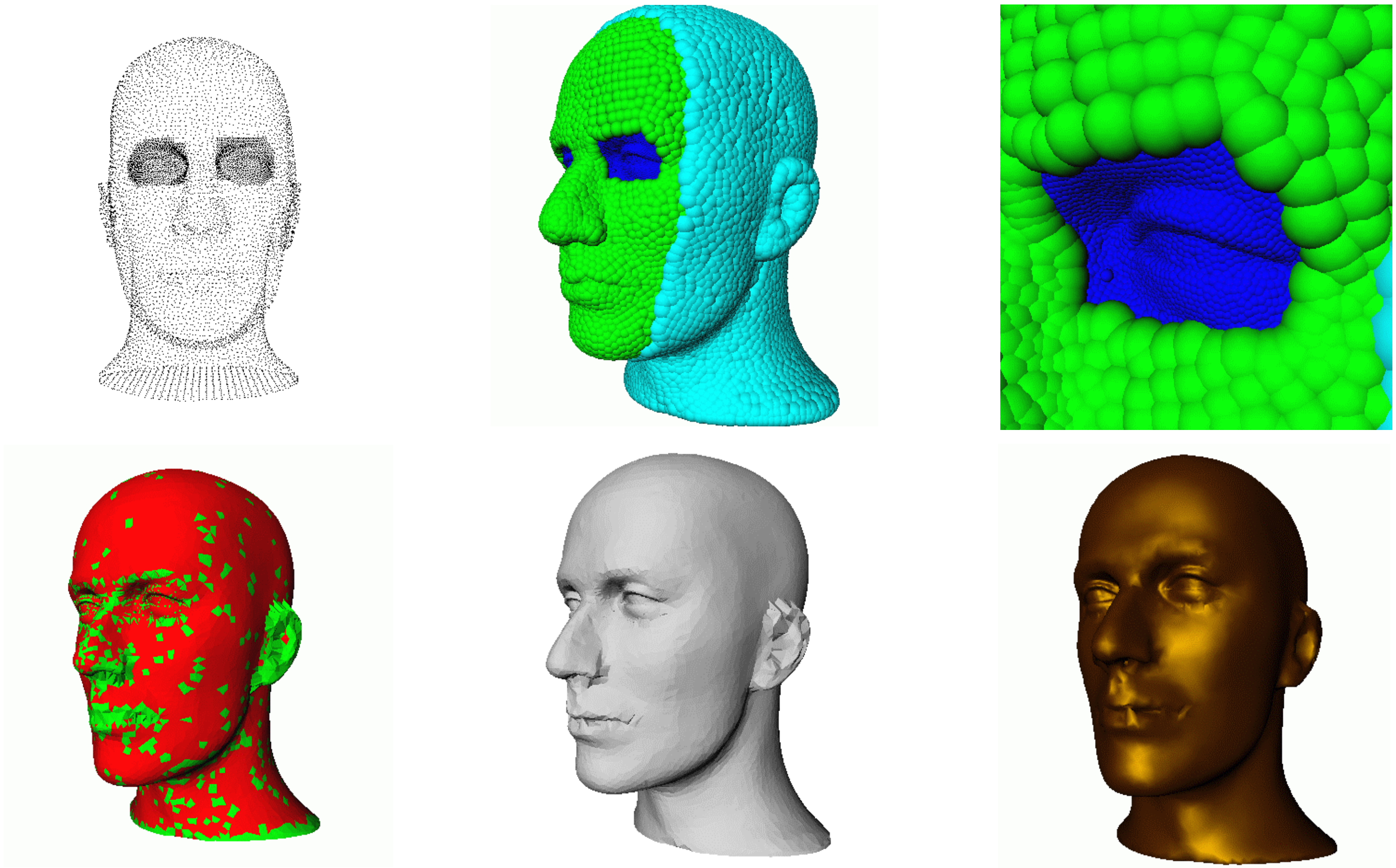

Connect-the-dots

- Inferring topology from proximity

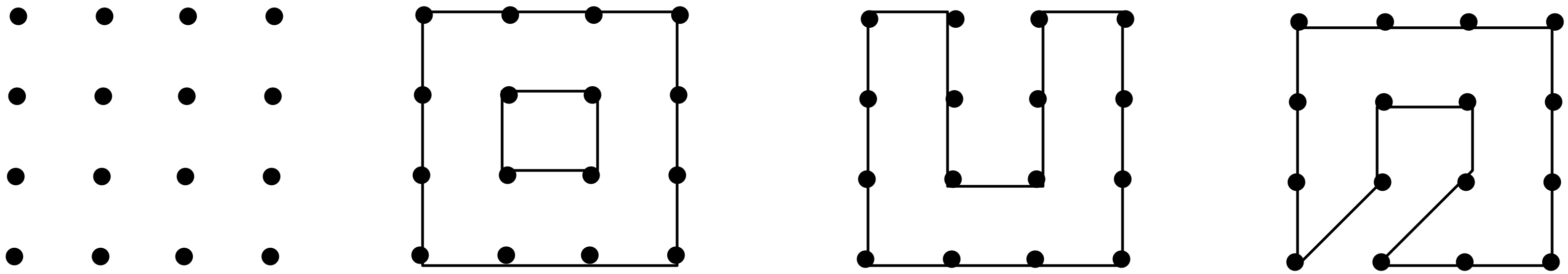

Reconstruction from points is in general an underconstrained problem

Sampling a 1-manifold

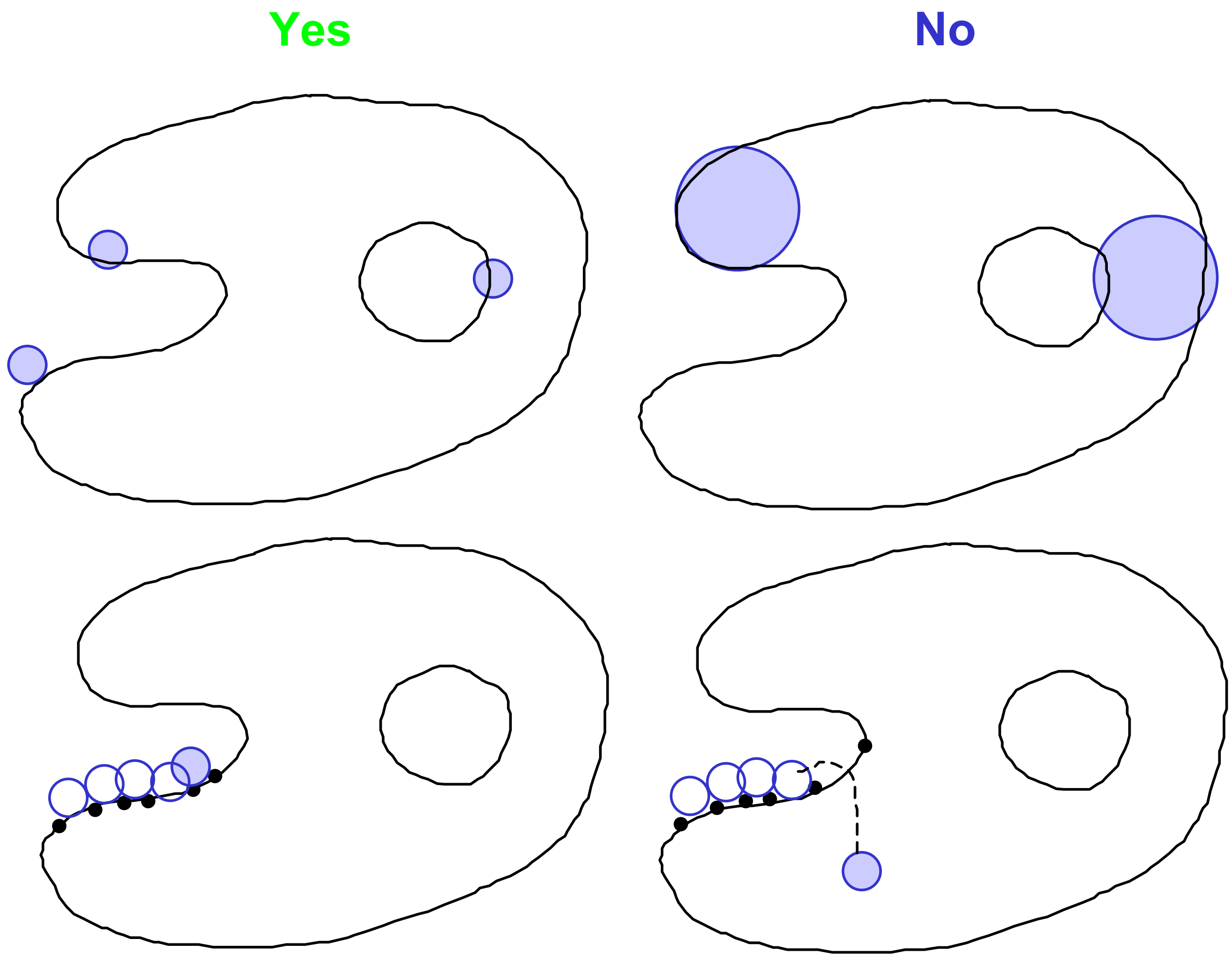

Neighborhood intersection property

Sampling density property

Sampling and Reconstruction Theorem (IJCGA'96)

- Let B be a compact 1-manifold without boundary, and S a sampling. If
- 1. for any closed disk D of radius r, $B \cap D$ is either (a) empty, (b) a single point, (c) an interval;
- 2. an open disk of radius r centered on B contains at least one point of S
- then the alpha-shape W_α, $\alpha = r^2$, is homeomorphic to B and

$$\max_{p \in W_\alpha} \min_{q \in B} \| p - q \| < r$$

Feature Preserving Reconstruction of CAD Models

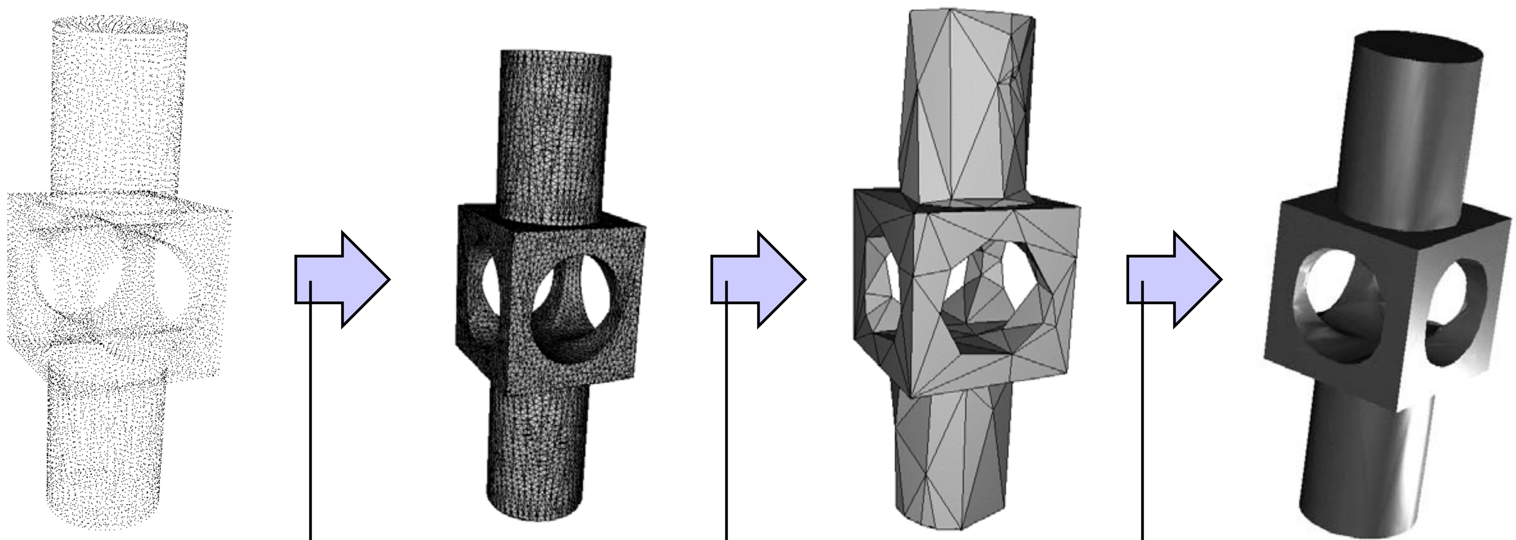

Points → **Triangle mesh** → **Reduced mesh** → **Smooth model**

3D Delaunay tri. and α–solid

Mesh reduction

A-patch fitting

Feature Surface Fitting

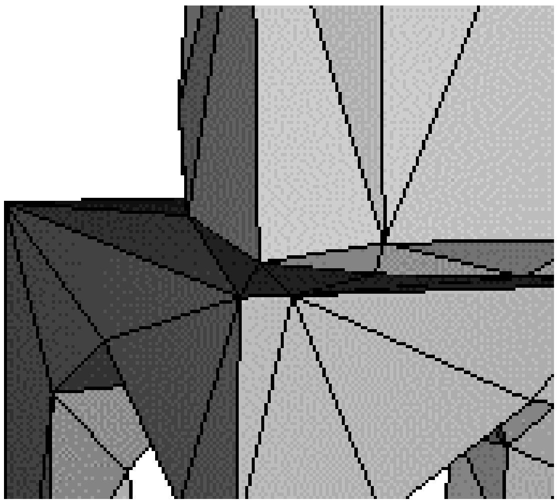

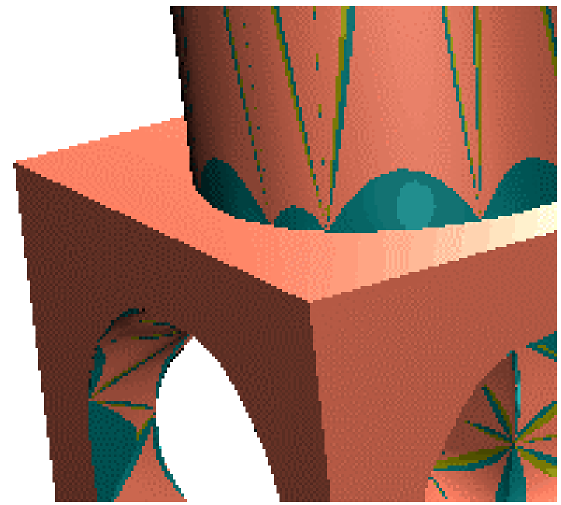

- Uses cubic A-patches (algebraic patches)
- C^1 continuity

- Sharp features (corners, sharp curved edges)
- Singularities

Feature Preserving Model Reconstruction

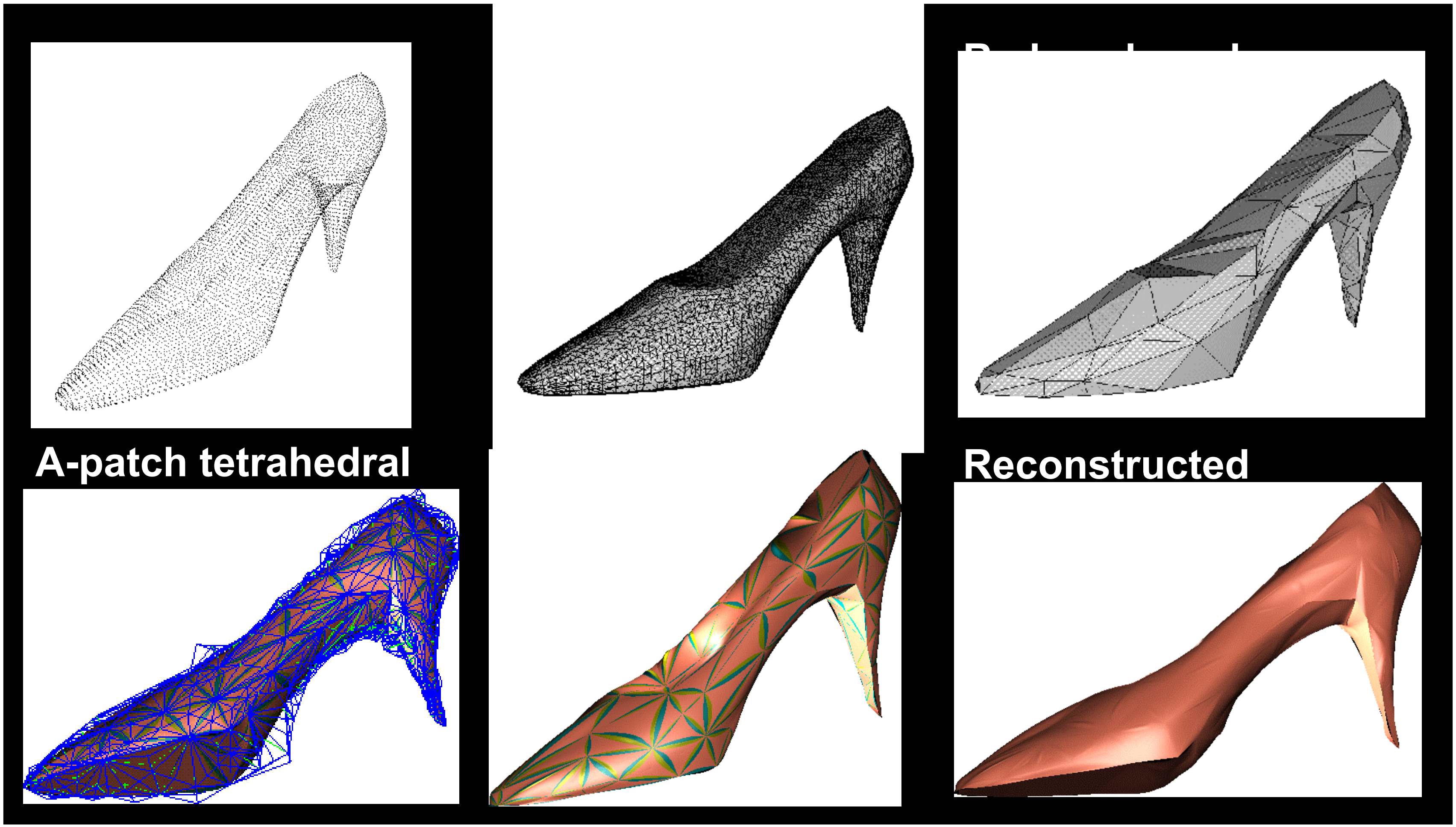

Sharp Features Reconstruction:

Further reading

- **Line integral convolution**
- Brian Cabral and Leith Casey Leedom, Imaging vector fields using line integral convolution, Proceedings of the 20th annual conference on Computer graphics, p 263-270

- **Fast Line Integral Convolution**
- Detlev Stalling and Hans-Christian Hege, Fast and resolution independent line integral convolution, Proceedings of the 22nd annual ACM conference on Computer graphics, p 249-256
- Rainer Wegenkittl and Eduard Gröller, Fast oriented line integral convolution for vector field visualization via the Internet, Proceedings of the conference on Visualization '97, p 309-316

- **Flow Fields**
- Han-Wei Shen; Kao, D.L., A new line integral convolution algorithm for visualizing time-varying flow fields, Visualization and Computer Graphics, IEEE Transactions on , Volume: 4 Issue: 2 , April-June 1998, Pages 98 -108
- Interrante, V.; Grosch, C., Strategies for effectively visualizing 3D flow with volume LIC, Visualization '97., Proceedings , 1997 p 421 -424,
- Wegenkittl, R.; Groller, E.; Purgathofer, W., Animating flow fields: rendering of oriented line integral convolution, Computer Animation '97 , 1997 p 15 -21
- Forssell, L.K.; Cohen, S.D., Using line integral convolution for flow visualization: curvilinear grids, variable-speed animation, and unsteady flows, Visualization and Computer Graphics, IEEE Transactions on , Volume: 1 Issue: 2 , June 1995 p 133 -141
- Forssell, L.K.,Visualizing flow over curvilinear grid surfaces using line integral convolution, Visualization, 1994 p 240 -247

- **Others**
- Han-Wei Shen, Christopher R. Johnson and Kwan-Liu Ma, Visualizing vector fields using line integral convolution and dye advection, Proceedings of the 1996 symposium on Volume visualization, Page 63
- Verma, V.; Kao, D.; Pang, A., PLIC: bridging the gap between streamlines and LIC**,** Visualization 1999, p 341 -541
- Gerik Scheuermann, Holger Burbach and Hans Hagen, Visualizing planar vector fields with normal component using line integral convolution, Proceedings of the conference on Visualization '99, Pages 255-261
- C. Rezk-Salama, P. Hastreiter, C. Teitzel and T. Ertl, Interactive exploration of volume line integral convolution based on 3D-texture mapping, Proceedings of the conference on Visualization '99, Pages 233-240
- de Leeuw, W.; van Liere, R., Comparing LIC and spot noise**,** Visualization '98. Proceedings , 1998 p 359 -365
- Ming-Hoe Kiu; Banks, D.C., Multi-frequency noise for LIC, Visualization '96. Proceedings. , 1996 p 121 -126

Further Reading

- Bader(1990)- gradient fields in molecular systems.
- Bergman, Rogowitz, and Treinish(1995) - enhancing colormapped visualiztion.
- Gershon(1992) - Generalized Animation
- Jones and Chen(1994), Lorensen and Cline(1987), Wilhelms and Gelder(1990) - isocontours in 2d and 3d scalar data.
- Fowler and Little(1979) - detecting ridges and valleys.
- McCormack, Gahegan, Roberts, Hogg, Hoyle(1993) - detecting drainage patterns in geographic terrain.
- Interrante, Fuchs, and Pizer(1995) - enhancing surface displays
- Itoh and Koyamada(1994) - Isocontour extraction.
- Helman and Hesselink(1991), Globus ((1991), Asimov ((1993) - vector field topology.
- Yih ((1957), Kenwright, Mallinson ((1992) - dual stream functions

Further Reading

- J. Hultquist, Construcing stream surfaces in steady 3D vector fields, proceedings of visualization '92
- J. Van Wijk, implicit stream surfaces, proceedings of visualization '93
- Scheurman, Hagen, Rockwood, constructing degenerate vector fields, proceedings of visualization '97
- Bajaj, Pascucci, Schikore, scalar topology for enhanced visualization, proceedings of visualization '98

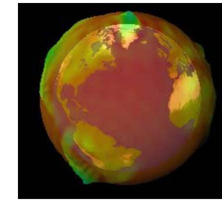

Computational Visualization

1. Sources, characteristics, representation

2. Mesh Processing

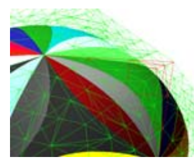

3. Contouring

4. Volume Rendering

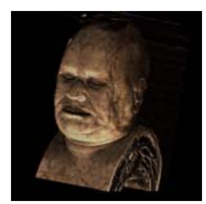

5. Flow, Vector, Tensor Field Visualization

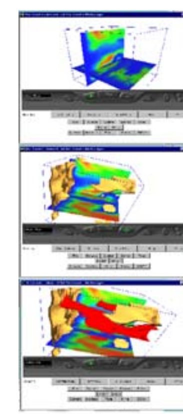

6. Application Case Studies